Advanced Composite Materials
Publication details, including instructions for authors and subscription information:
http://www.tandfonline.com/loi/tacm20

Overview of trends in advanced composite research and applications in Japan

Takashi Ishikawa

Version of record first published: 02 Apr 2012.

To cite this article: Takashi Ishikawa (2006): Overview of trends in advanced composite research and applications in Japan, Advanced Composite Materials, 15:1, 3-37

To link to this article: http://dx.doi.org/10.1163/156855106776829383

Adv. Composite Mater., Vol. 15, No. 1, pp. 3–37 (2006)

Also available online - www.vsppub.com

Review

Overview of trends in advanced composite research and applications in Japan

TAKASHI ISHIKAWA *

Aviation Program Director, Japan Aerospace Exploration Agency, 7-44-1, Jindaiji-Higashi-Machi, Chofu, Tokyo 182-8522, Japan

Received 28 November 2005; accepted 22 December 2005

Abstract—Recent research activities in advanced composites technologies conducted in Japan are reviewed and introduced. New research topics in reinforcing fibers described are low modulus pitch-based carbon fiber and PBO fiber. The second of these is very topical at the present time: nano-technology based composites use materials such as carbon nanotube, or carbon nano-fiber, or nanoclay. Because the Composites Technology Center in the Japan Aerospace Exploration Agency (JAXA) leads many new research fields in composites, the present review paper shows a slight bias towards the outputs of JAXA. The most remarkable outcome in this field at present is a compression strength improvement by loading cup-stack type carbon nano-fiber (CSCNF). Prepreg containing this CSCNF has been developed and has already been rerleased into the market. The third topic is related to newly developed high performance polymers including heat resistant polyimide, Tri A-PI and its family. The most recent product is a heat resistant polyimide that is highly soluble in some organic solvents; this material is suitable for preparation of imide wet prepreg. Composites fabricated through this prepreg route exhibit no voids and defects compared to the traditional amid-acid polyimide prepreg route. Another new topic in polymers is related to Japan's national project, radiation cure polymers and their processing. Electron beam cure, ultra-violet cure and visual light cure resins and their processing technologies have been developed in this national project. The next topic is a development of the low cost composites technology mainly for aircraft components. JAXA's activities related to this field are introduced first based on two new key technologies — Z-anchor® and stitching. New findings about the mechanism of interlaminar reinforcement by stitching are slightly focused. Finally, remarkable theoretical findings about composite mechanics in recent years are described. A clarification of mechanics of compression after impact behavior by using a newly developed cohesive zone element is reviewed first in this category. Matrix crack growth theories in the laminae adjacent to the initially cracked layer are introduced next where a motivation of this research is a cryogenic composite tank for future space transportation systems. The final topic is a development of the theory of structural health monitoring by using small diameter FBG sensor. By an evolution of these theories structural health monitoring has almost reached the level of practical applications.

Edited by the JSCM.

*E-mail: isikawa@chofu.jaxa.jp

Keywords: New fiber; nanotube; new polymer; low cost technologies; new theoretical findings.

1. INTRODUCTION

It is a very fortunate situation that *Advanced Composite Materials,* which used to be the official journal of the Japan Society for Composite Materials (JSCM), has become the official publication controlled equally by the Korean Society for Composite Materials (KSCM) and JSCM. In order to celebrate this re-inauguration of the journal, the joint editorial board has decided to publish two review papers about composite research trends in each country. The author representing the Japanese side (TI) is very pleased and honored to be given such a great opportunity. So, this article is not only a scientific review of the composite research trends but also a proof of the friendship in composite research and development fields between two countries which has been fostered for a long time.

This review article covers wide aspects of advanced composites research trends conducted in Japan. However, an emphasis is naturally placed on aerospace related research subjects reflecting the author's interest and affiliation (Japan Aerospace Exploration Agency: JAXA). Moreover, the referred topics will be biased slightly into JAXA in-house research because he is familiar with the recent interesting results there. The author would like to apologize to the reader about this bias first. Of course, the fact that the length of the article is limited is another constraint on the content coverage. Thus, he tries to concentrate on new, topical, fascinating and important topics in composite research and development in various engineering fields as much as possible. If this article can stimulate many brilliant young composite researchers in both countries, the author fully accomplishes his aim for the publication.

2. FIBERS AND REINFORCEMENTS

The most important reinforcing fiber in advanced composites is, of course, carbon fiber which is roughly classified into two groups — high strength fiber and high modulus fiber. Japan dominates in commercial production of carbon fibers on the world wide scale, as shown in Fig. 1. Development directions of carbon fiber have been clearly split corresponding to the above two groups in these past twenty years, as shown in Fig. 2 [1]. However, growth in the fiber properties towards high strength (moving upwards on the graph) and high modulus (moving right on the graph) directions seems to have become saturated in recent years. Among such trends, a newcomer is a group of low modulus fibers based on pitch as indicated in Fig. 2 by solid circle symbols. This type of carbon fiber is an invention of Nihon Graphite Fiber Co. Ltd. [2] in Japan. One unique feature of these fibers is a high strain-to-failure in compression in unidirectional composites made of these fibers [2] as shown in Table 1. Due to this unique feature, these fibers can be applied

Figure 1. Worldwide production of carbon fiber and Japan's domination.

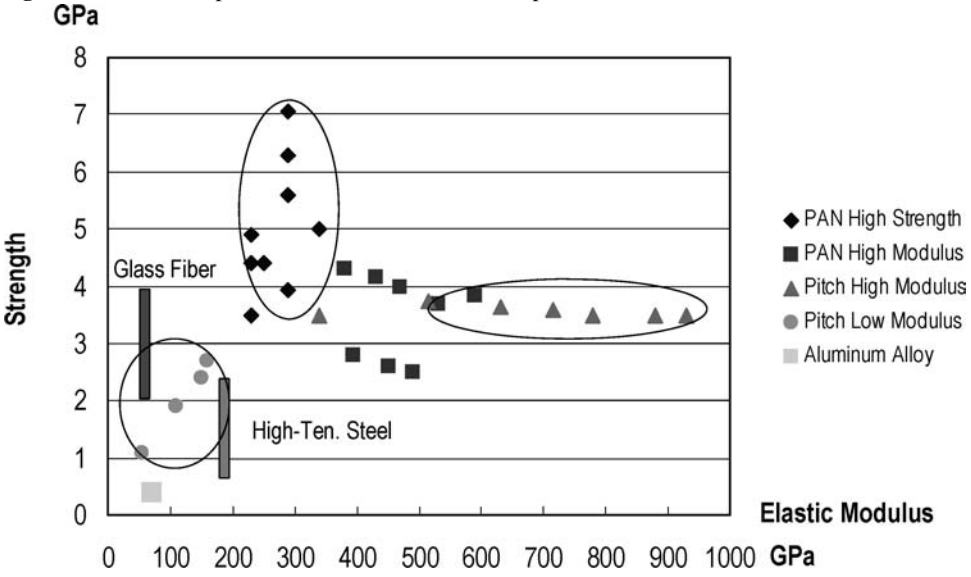

Figure 2. Development trends in carbon fiber properties.

to unexpected components. An example of application of low modulus pitch fiber to the shafts of golf clubs in order to increase bending failure load [2] is shown here. A schematic view of the shaft, its lamina stacking sequence and results of three point bending impact [2] are shown in Fig. 3, where 'T700S pipe' or 'XN-05 pipe' indicates that the outer reinforcing layer consists of each nominated unidirectional lamina, respectively (3 plies or 4 plies corresponding to lamina thickness). The other lamina arrangement is as follows: the inner bias layers consist of Toray M40J 4 plies and the middle and load-carrying straight layer consists of Toray T800H 3 plies, where all matrices are epoxy resin. It is very clear that XN-05 pipe shows quite higher bending load, bending deflection and stored energy before failure, which is the most important for the golf club shaft, although the compression strength of T700S is much higher than XN-05 according to Table 1. This phenomenon is

very interesting and is worth being studied. The authors of ref. [2] conducted 3D finite element analysis and concluded that the compression stress in the thickness direction at the loading point in the 3-point bending may increase the compression strength of load carrying T800H lamina if the outer layer compression failure does not happen due to its large strain-to-failure. Although some further study might be needed because the actual situations in golf club shafts or fishing rods are cantilever

Table 1.
Tensile and compressive properties of unidirectional carbon fiber/epoxy laminate

		Pitch-based low modulus CF			PAN-based CF	
		XN-05 CFRP	XN-10 CFRP	XN-15 CFRP	T700S CFRP	T800H CFRP
Tensile properties						
Tensile strength	MPa	650	1050	1400	2650	2845
Tensile modulus	GPa	34	72	93	127	150
Strain to failure	%	1.8	1.5	1.4	1.8	1.6
Compressive properties						
Compressive strength	MPa	880	1070	1150	1470	1570
Compressive modulus	GPa	32	64	85	123	147
Strain to failure	%	2.9	2.1	1.8	1.4	1.0

Note: The strength and modulus were normalized to a fiber volume fraction of 60%.

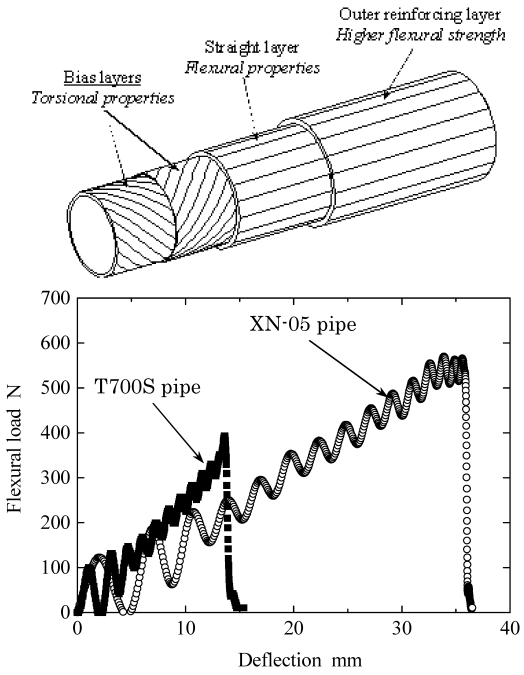

Figure 3. Schematic of golf club shaft wrapped by low modulus pitch fiber and its impact response.

end loading instead of three point bending, the experimental findings and analysis are very encouraging. In the case of components based on cylindrical geometry of a small diameter and predominantly bending loads, similar situations can be expected according to this discovery. The phenomenon might be referred to as 'structural hybrid effect' in a cylinder. Due to such a property, this fiber will be highly enhanced in the sporting goods market.

Another new trend in long fibrous reinforcement is 'PBO' fiber where PBO is an abbreviation of poly(*p*-phenylene benzo-bis-oxazole). Although this fiber was originally invented in the USA, a Japanese company, Toyobo Co. Ltd., bought the license and produces it commercially in Japan. A feature of this fiber is the very strong tensile strength, which is better than Kevlar® fiber as the organic material, as shown in Fig. 4 [3], although the stress–strain plot of high strength carbon fiber in this figure is quite intentionally low. Other features of this fiber are resistance to fire and flame with a LOI (Limited Oxygen Index) value of 68 in comparison to the value of 58 for carbon fiber and 30 for aramid fiber and great impact tolerance due to high energy absorption capacity. So, possible application fields of this fiber are tension structures, such as membrane of airships or civil structures for retrofitting. An example of applications to civil field components is introduced here. An upper portion of Fig. 5 [4] indicates the schematic of strengthening technique of a concrete beam by pre-stressed PFRP (PBO Fiber Reinforced Plastic) sheets. The PBO fiber sheets are first stretched to a percentage of pre-stress, then coated with epoxy resin on-site and bonded to the structural concrete surface. After curing, the tensile load is released and the pre-stress is transferred to the concrete beam structure. The key technology responsible for the success of this material is the bond at the interface. To achieve a perfect bond, an air bag system with vacuum facility is developed for construction site applications. Moreover, the shear stress concentrations at two ends are usually the cause of debonding, and attributed to the high loads due to pre-stressing forces. Therefore, reduction of shear stress concentration can be accomplished by gradually releasing the pre-stressing forces

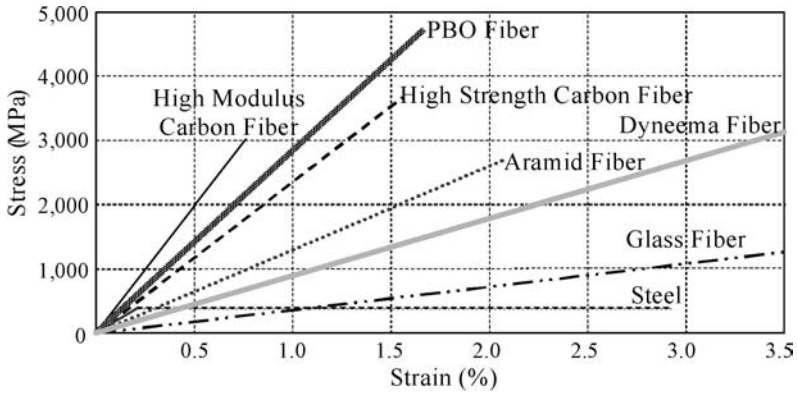

Figure 4. Stress–strain relationships of various fibers.

at both ends and by reducing the number of layers in composites used at the ends together with FRP U-anchors or bolt anchorage with bonded steel plates. The lower portion of Fig. 5 [4] shows typical load–deflection curves of 10 m long concrete girders with pre-stressed PBO fiber sheets at different pre-stress levels. The control girder without external reinforcement failed due to yielding of tensile steel followed by concrete crushing. The girder strengthened by three-layer PBO sheets without pre-stressing exhibited the similar bend-over point to the control, but gained significant strain hardening after the yielding of steel. With pre-stressing, the linear proportional limit was increased by 45% and the ultimate load by 65%. A high percentage of pre-stressing could effectively change the failure mode from debonding to PBO tensile rupture, leading to a significant increase in load-carrying capacity. This technology and PBO fiber show high potential of increasing load-carrying capacity of civil structures such as the bridge girders.

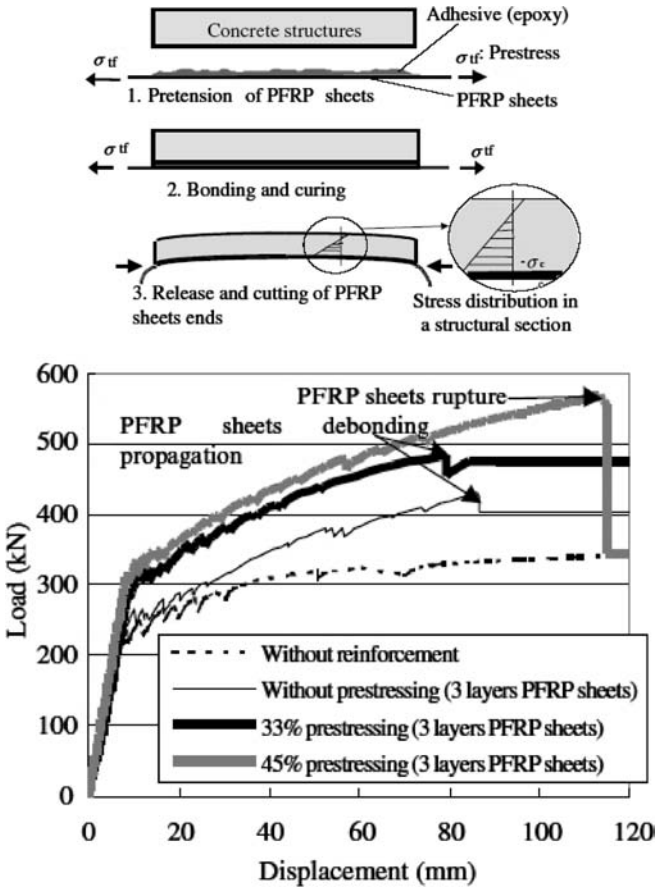

Figure 5. Load–deflection curve of concrete girder of 10 m span with pre-stressed PFRP.

3. NANO-TUBES, NANO-FIBERS AND NANO-FILLERS

A big boom of nanocomposites research has landed also in Japan. As a virtual 'center of excellence' in composites technology there, ACE TeC of JAXA has led pioneering sections of nanocomposites research, particularly in mechanical properties oriented applications. An overview of research activities related to nanocomposites in ACE TeC will be given first and some remarkable results will be introduced briefly.

The first example is a Carbon Fiber Reinforced Composite (CFRP) laminate using epoxy resin stiffened by carbon nanotubes (CNT). It is well known that CNT exhibits extremely high elastic modulus and strengths. One trend in CNT application as composite reinforcement is direct dispersion like chopped fiber in polymer with an alignment as parallel as possible, which is considered as two-phase material of CNT and polymer. Although it looks like a proper way of obtaining CNT-reinforced composites, alignment of CNT with uniform spatial dispersion in resin is not an easy task. ACE TeC pursues another route for CNT reinforced composites of three-phase material — CNT, polymer and conventional carbon fiber (CF). In this idea, CNT can be regarded as a modifier of matrix resin for increasing its mechanical properties. In this trial, the CNT used is unique, and should be referred to as carbon nanofiber (CNF): Carbere®, made by GSI CREOS Corporation in Japan [5]. They refer to this product as cup-stack nanofiber (CSNF). A schematic illustration [5] of such CSNF is shown in Fig. 6 where conical graphene sheets are accumulated like a stack of paper cups and their outer diameter is in the range of 80 to 100 nm with 15 nm wall thickness, which is rather larger than usual CNT. The mechanical properties of this CSNF are compared in Fig. 7 where common carbon fiber data are plotted [5]. Two types of CSNF were employed in the difference of aspect ratios, i.e. fiber length of 500 nm to 1 μm (AR10) and fiber length of 2.5 to 10.0 μm (AR50), respectively. These two types of CSNF are dispersed to Epikote® 827 epoxy resin by the company and they can supply the dispersed

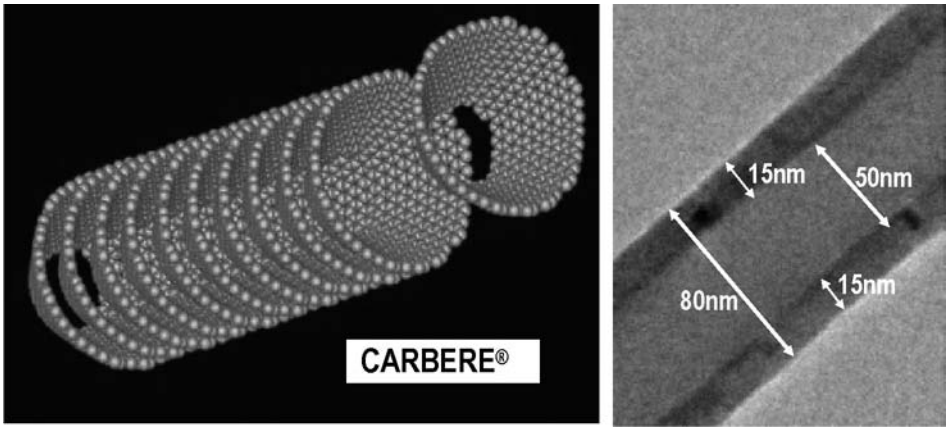

Figure 6. Schematic illustration of cup-stack type carbon nanofiber and its dimensions.

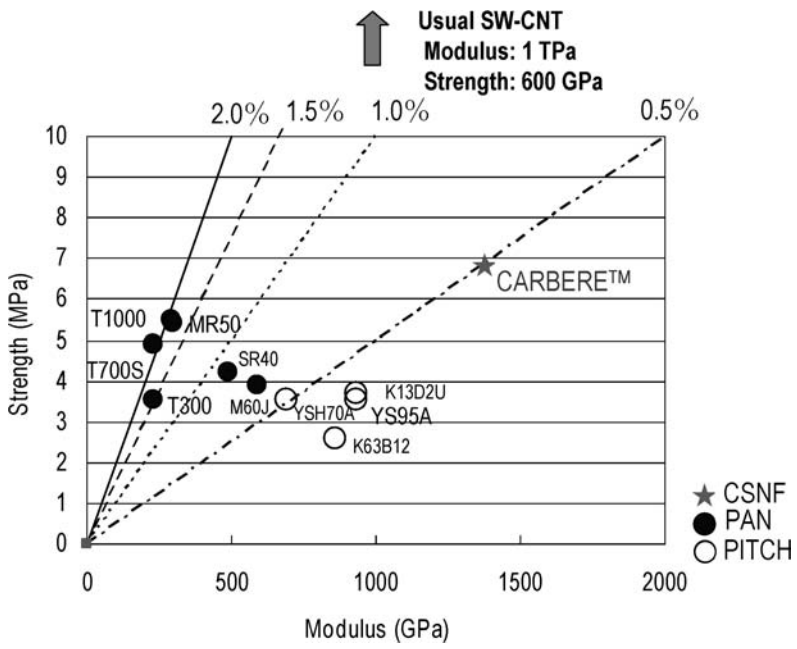

Figure 7. Strength and modulus plot of cup-stack type carbon nanofiber.

compound of high CSNF weight content and this epoxy. At the first trial stage, a manual fabrication process of the composite plates by impregnation of the diluted compound by the same epoxy into dry carbon fiber fabrics (Torayca CO6343: T300/plain weave) was employed followed by the hot-press curing.

Compression strength improvements around 15% in the three-phase composites by a loading of CSNF in comparison with the control case of no CSNF are shown in Fig. 8 as the typical example of this stage [5] where all strength data are normalized by the control data. The most efficient case, 5% loading of the weight of the resin with AR 50 CSNF, is marked by a circle in this figure. By stimulating such promising results, the supplier company of CSNF, GSI-Creos, decided to develop prepreg systems containing dispersed CSNF [6] in order to obtain more stable mechanical properties than manual fabrication processes. Another key issue in the prepreg development is an optimization of the aspect ratio of CSNF. Although the details of this process belong to the company and cannot be disclosed, one advantage for a good dispersion is many numbers of edges of graphene sheets appearing on the CSNF surface. Such edges may help to increase interaction between CSNF and polymer due to this cup-stack nature. A good dispersion of CSNF is suggested in the microscopic sectional view of Fig. 9 for the three phase composites through the prepreg route [6]. Compression strength improvement in these three phase composites by the prepreg is more remarkable than manually impregnated cases as shown in Fig. 10 [6]. In this T–700 CF UD prepreg case, the compression strength in the fiber direction is improved by some 25% in comparison with the control (no CSNF) case. However as shown there, the elastic modulus in compression of

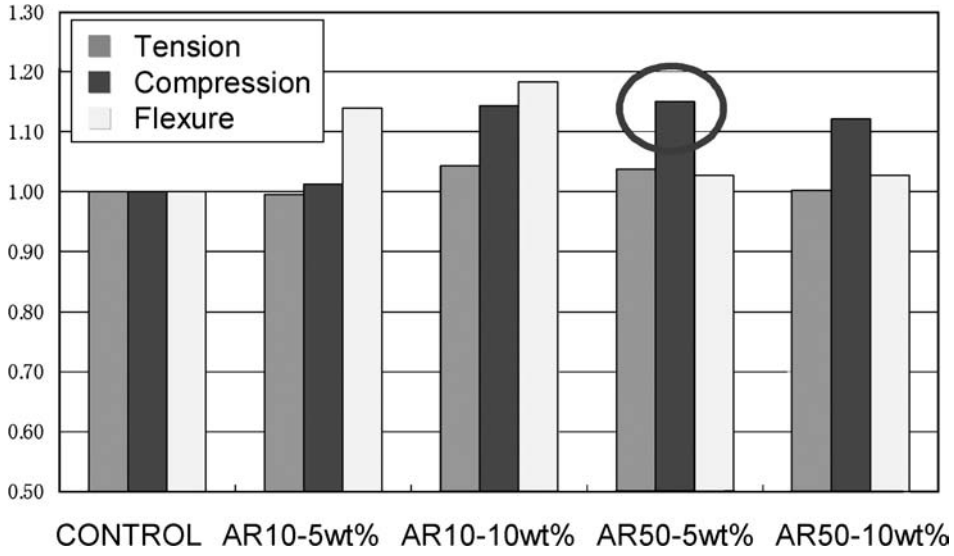

Figure 8. Compression strength increase in CSNF/epoxy/CF three-phase composites.

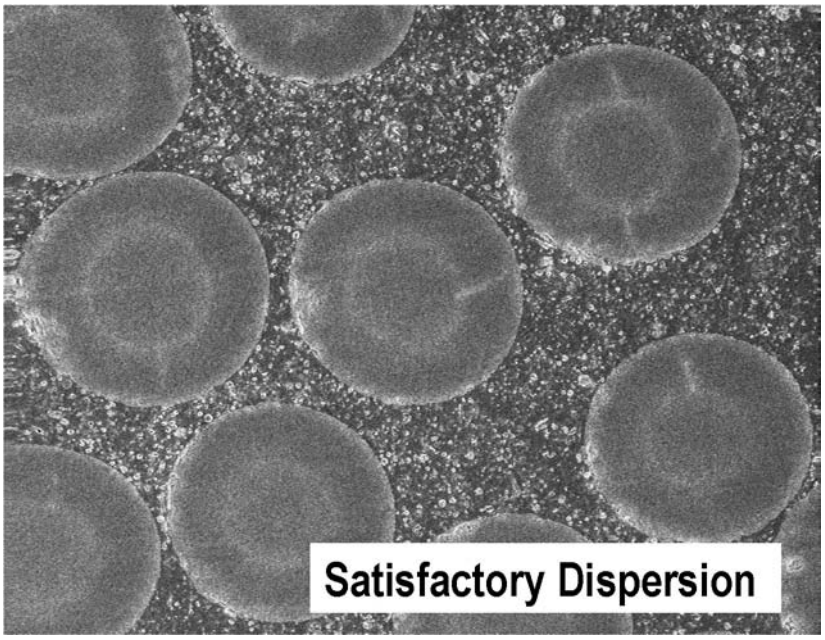

Figure 9. SEM view of CSNF/epoxy/CF three phase composites by prepreg route.

this composite is not affected as naturally expected. These prepreg systems are considered to be very potential and they are now available in the composite raw material market. Moreover, their applications have been started to the sporting goods in Japan.

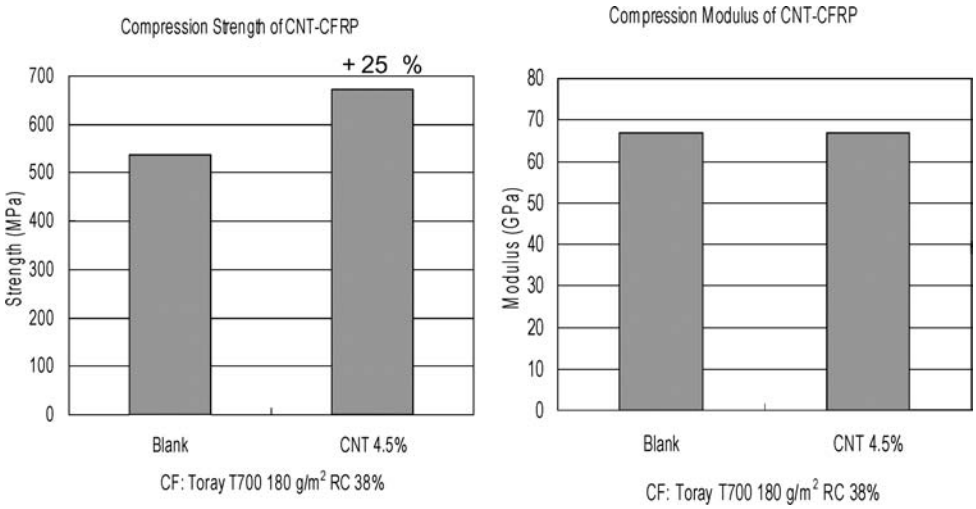

Figure 10. Compression strength and modulus in CSNF/epoxy/CF three-phase composites by prepreg route (T700, 180 g/m^2 fiber aerial weight, CNT%: volume content).

The second research topic concerning nanotechnology composites in ACE TeC/JAXA is an improvement of heat resistance of high temperature polymer [7] by loading of multi-wall carbon nanotube (MW-CNT). In this attempt, a baseline polymer itself is one of the ever-best high temperature polymers, Triple A Polyimide (TriA-PI), which shows much better heat resistance than NASA standard PETI-5. The detail of this resin will be explained in the next section on newly developed polymers. The final purpose here is to increase heat resistance such as glass transition temperature by adding MW-CNT to this polymer. The MW-CNT adopted in this attempt is fabricated through CVD technique by Carbon Nanotech Research Institute Inc. (CNRI) in Japan [7]. The SEM picture of this MW-CNT is shown in Fig. 11 where its diameter and lengths show the scatter of 20 to 100 nm and several μm, respectively. Chosen loading weight fractions of MW-CNT are as follows: 0, 3.3, 7.7 and 14.3%. Because the imid-oligomer is solid at room temperature, MW-CNT is added to imid-oligomer powder and mechanically blended by a ball mixer (Route (I)). Then the mixture is consolidated by using a hot-press for an hour at 370°C. Another processing route is the liquid route in an amid acid/NMP solution with some chemical reactions including imidization (Route (II)) although a description of the details is not given here. The obtained material is a two-phase composite if we follow the previous terminology. Dynamic viscoelastic properties were measured for the obtained composites by a dynamic mechanical analyzer (DMA: Q800 of TA Instruments Corp.) in the single cantilever bending method and static tensile properties were measured with a small coupon of 5 mm $\times$ 1.1 mm $\times$ 80 mm (width $\times$ thickness $\times$ length). Increases in the glass transition temperature (T_g) based on the dynamic mechanical analyzer are shown in Fig. 12, where T_g defined by initiation of the storage modulus reduction is 333°C for the

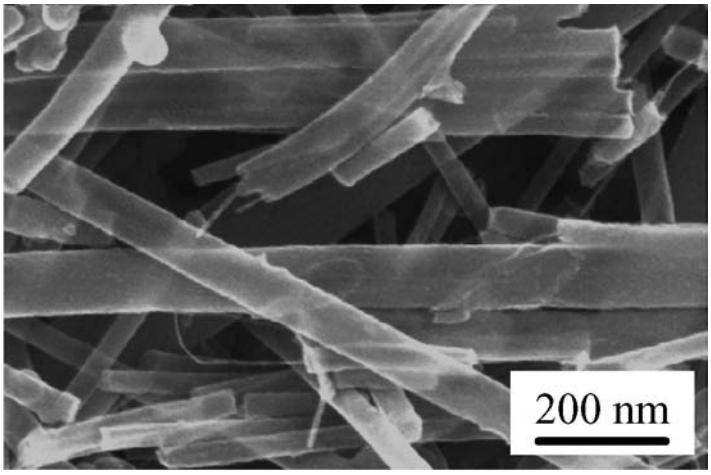

Figure 11. Used multi-wall carbon nanotube for raising heat resistance of new polyimide.

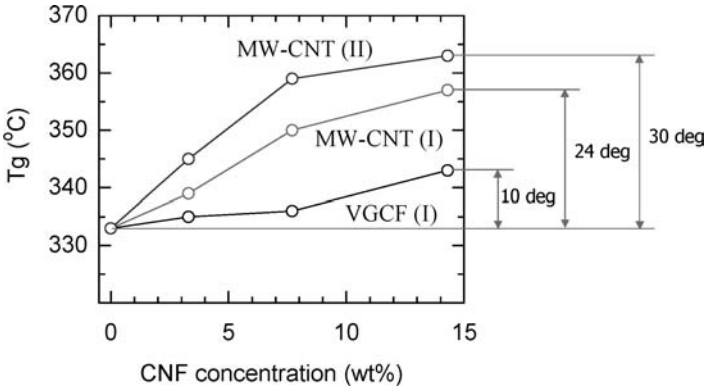

Figure 12. Upgrading of glass transition temperature (T_g) by loading of multi-wall carbon nanotube to new polyimide (Tri A).

neat resin (TriA-PI) and 363°C for composite with 14.3% weight MW-CNT through Route II (the liquid route). A remarkable increase of 30° in T_g is identified [7]. The reason why dispersed MW-CNT increases the heat distortion temperature may be explained as follows: the dispersed MW-CNT impedes the molecular motion in polyimide network at elevated temperature. However, more research work would be required to prove that the suggested phenomenon is a true cause of higher T_g. Although static properties are obtained, discussions are not given here. The other property improvements in this material are that MW-CNT shows some potential for controlling electric conductivity and electro-magnetic wave absorbability.

The third research topic concerning nanocomposites conducted in ACE TeC/JAXA is nano-clay dispersed composites [8] for improving gas barrier properties. This research topic is a basic part of the future cryogenic composite tank as a liquid

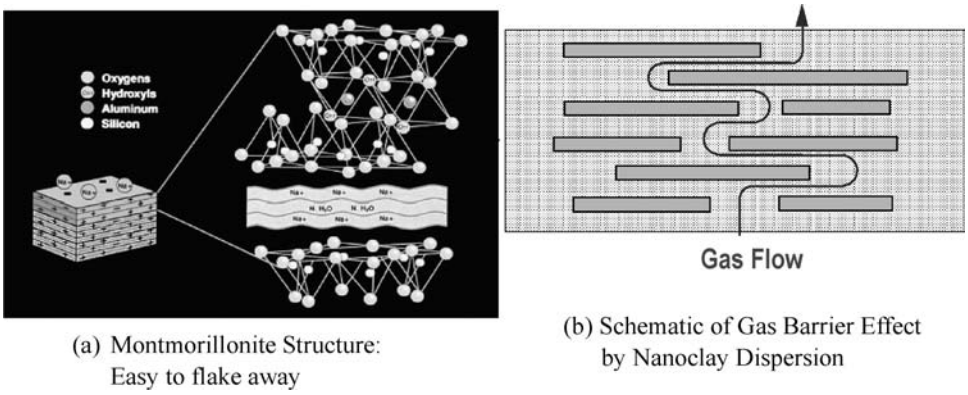

Figure 13. Schematic of montmorillonite structure and possible gas barrier effect.

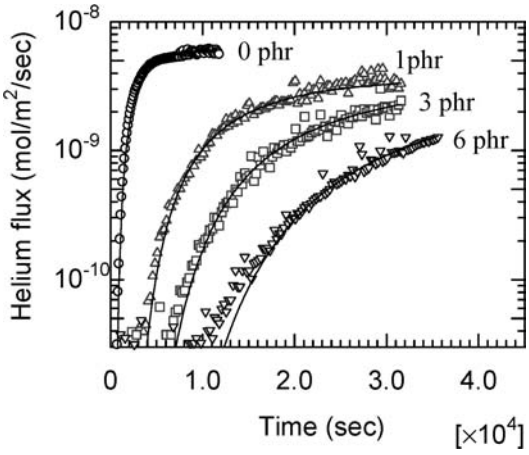

Figure 14. Effect of nanoclay loading upon helium flux history.

hydrogen reservoir for space vehicles. The nano-clay systems used are two types of modified montmorillonite, Nanofil-32 and Nanomer, and schematic illustrations of their nano-structure and their function are shown in Fig. 13 [8]. The surface modified clays are amenable to make organic/clay nanocomposites because of the weak bonding force between layers of montmorillonite. Dispersion occurs in the compounding operation and the case where complete dispersion occurs is referred to as exfoliation. When nano-clays are exfoliated completely in a resin matrix, the result is a perfect nanocomposite. Typical diameter and thickness of exfoliated clay in the nanocomposites is about 10 μm, and 1 nm, respectively, while the aspect ratio of this exfoliated clay was assumed to be 0.001. In this study, the base resin is a typical less viscous epoxy of Epikote 807 for better dispersion. Figure 14 depicts the effect of nano-clay loading upon helium gas permeability in the present composites obtained by a helium leak detector [8]. If we convert the data into the diffusion coefficients and compare the experimental value and the theoretical

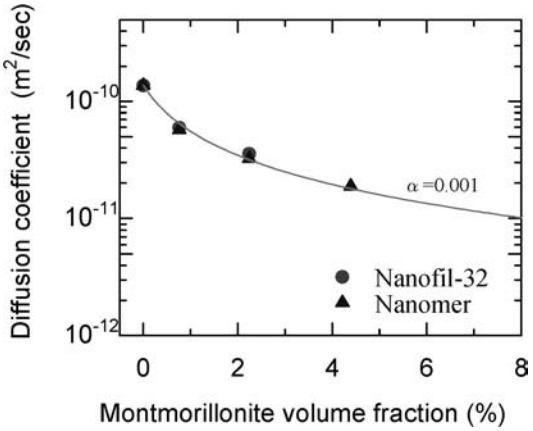

Figure 15. Experimental helium diffusivity and numerical results based on Hatta Taya Theory.

predictions, the plots look like Fig. 15 where the diffusivity of montmorillonite is assumed to be 1.0×10^{-13} m^2/s, which is about one-thousandth of the epoxy resin (1.37×10^{-10} m^2/s). It can be seen that a loading of the nano-clay of about 4 vol% (about 6 wt%) reduces the diffusion coefficient to 1/10, and that the theoretical predictions based on the aspect ratio of 0.001 agree well with the experimental results. These nano-clay composites show a high potential for future space vehicle materials.

4. NEWLY DEVELOPED POLYMERS

In this section, the main topic to be introduced is a new heat-resistant polyimide resin group developed in Japan. The first product, which is a new phenylethynyl terminated polyimide based on the reaction of asymmetric type (a-) BPDA, diaminine, and PEPA, was invented by Yokota *et al.* of JAXA in 1999 and published in 2001 [9]. Its chemical description is shown in Fig. 16 where the characteristics of this polyimide are amorphous, asymmetric, and addition type. Thus, this polymer is referred to as 'Triple A–Polyimide', or briefly 'Tri A-PI', which is already described in the previous section as the baseline polymer for carbon nanotube modification for T_g increase. So, its high T_g is indicated in Fig. 12 as a null MW-CNT content case. Not only because of its high T_g and thermo-oxidative stability, but also because of its favorable mechanical properties, large strain-to-failure of a neat resin of 12% [9], this polymer becomes an attractive candidate for matrix material of high temperature polymer composites with high toughness. This large strain-to-failure may be brought about by its asymmetric structure. It is now already commercially available as 'Upilex AD' by Ube Industries Ltd. Probably, the only one drawback of this resin, which is also the universal defect in all available polyimide polymers, is a by-product of H_2O during the final imidization of the precursor of poly(amide acid) solutions in the prepreg. This water becomes vaporized during the curing process

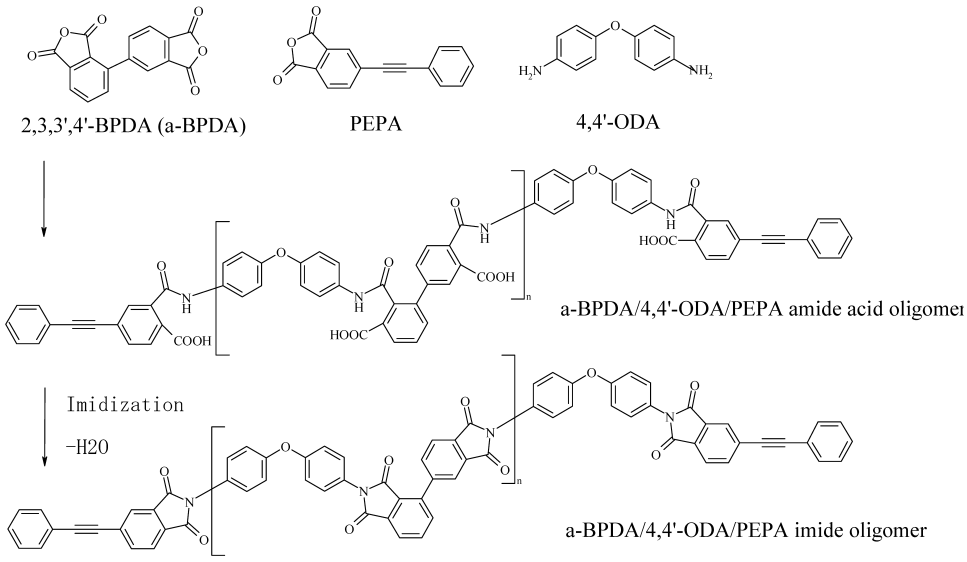

Figure 16. Chemical structure of 'Triple A Polyimide' invented by Yokota.

of composites and a possible source of voids. Hence, special precautions are required in the curing process in order to obtain good quality composites. Even if the preparation of imide solution prepreg is intended, it cannot be prepared because the solubility of imide oligomers is less than 20 wt% in N-methyl-2-pyrrolidone (NMP) or other solvents and the solution is often set to gel.

The second product to be introduced is aimed to solve thoroughly the above drawback. In order to do so, improvement of solubility and solution stability of imide oligomers maintaining high thermal resistance have been introduced. The key idea is an introduction of fluorenylidene groups into the Tri A-PI structure [10] and a schematic of the synthesis is shown in Fig. 17. Although the main structure of Tri A-PI is 2,3,3′,4′-biphenyltetracarboxilic dianhydride (a-BPDA) and 4,4′-oxydianiline (4,4′-ODA) as shown in Fig. 16, the key monomer introduced is 9,9-bis(4-(4-aminophenoxy)phenyl)fluorene (BAOFL) and its ratio to 4,4′-ODA is controlled by maintaining 4-phenylethynylphthalic anhydride (PEPA) termination [10]. The synthesized imide oligomers show excellent solubility of more than 40 wt% in aprotic polar solvents such as N-methyl-2-pyrrolidone (NMP), N,N-dimethylacetamide (DMAc) and γ-butyrolactone (GBL) at room temperature. The solubility is sufficient to prepare the imide solution prepreg and the stability of solution is good enough. By introducing BAOFL, T_g and strain-to-failure of neat resin film become slightly lower compared with the no BAOFL case (Tri A-PI). However, reduction of these two properties remains within a permissible range as composite matrix. Imide solution prepreg was prepared from o-BAOFL-50 imide oligomer solution in GBL. Figure 18 shows TGA curves of (a) the o-BAOFL imide solution prepreg using GBL and (b) the TriA-PI (o-BAOFL-0) amide acid solution prepreg using NMP [10]. Most of the volatile material was removed at 150°C in

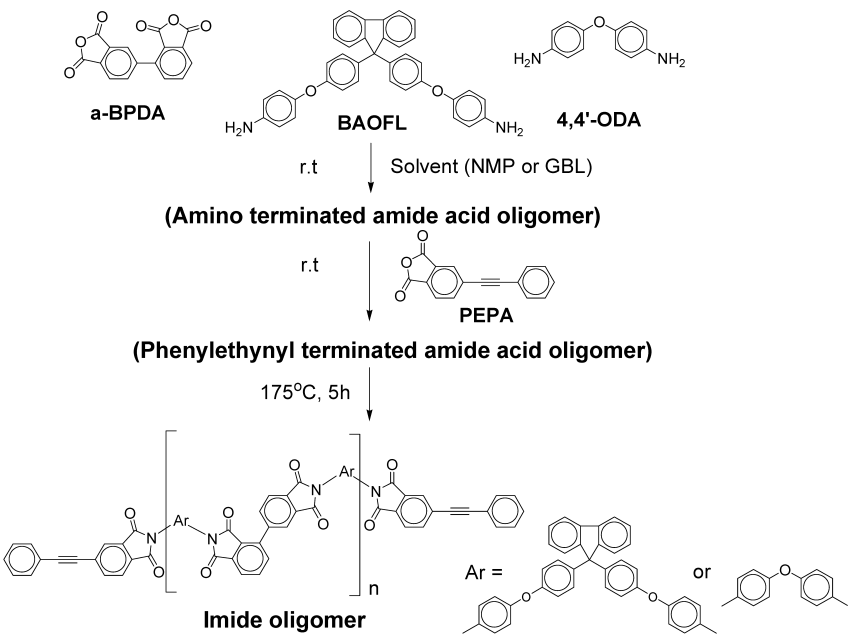

Figure 17. Synthesis of the additive imide oligomer containing fluorenylidene groups.

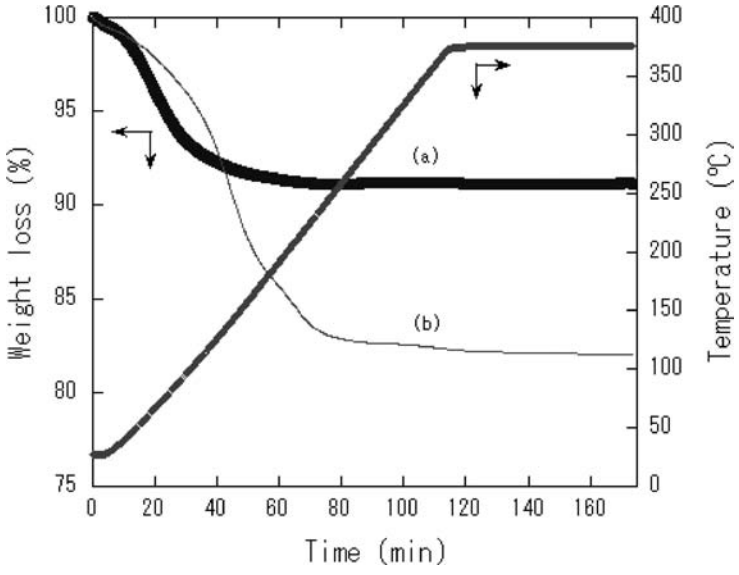

Figure 18. TGA curves of imide and amide acid solution prepregs: (a) o-BAOFL-50 imide prepreg (plain woven fabric) from GBL solution ($V_c = 14\%$); (b) TriA-PI (o-BAOFL-0) amide acid prepreg (unidirectional) from NMP solution ($V_c = 23\%$).

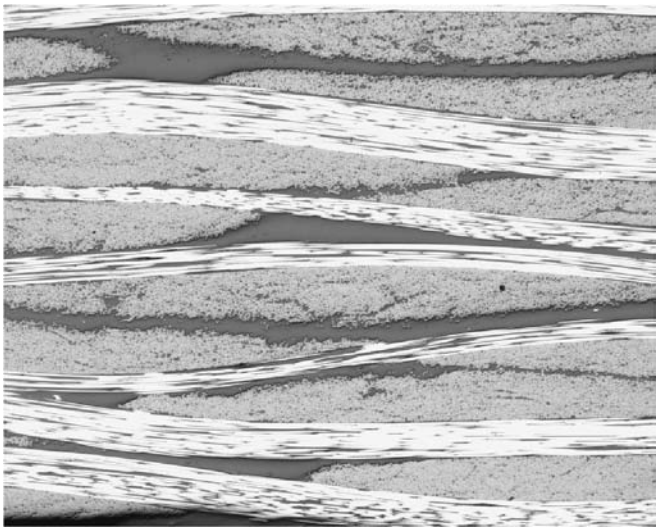

Figure 19. Optical micrograph of the o-BAOFL-50 polyimide/carbon fiber composite.

the case of the imide prepreg, whereas the volatiles of amide acid prepreg (NMP and water) were continued to evaporate to 250°C. The risk of void generation in composites will be reduced by using imide solution prepreg because the volatiles are more removable at low temperature. Finally, polyimide/carbon fiber composite was fabricated from the o-BAOFL-50 imide solution prepreg by two steps. First, the solvent was removed at 230°C for 3 h in an air oven. The prepregs were laid-up and vacuum-bagged, and then cured at 370°C for 1 h in an autoclave. The resulting composite was good quality as determined by C-scan. The optical micrograph of the composite section shown in Fig. 19 exhibits no voids or matrix cracks [10]. The T_g of the cured composite was 332°C and high heat resistance is confirmed with very favorable advantages of easy handling and wide processing window. It is certain that composites with this resin matrix will be one candidate to replace titanium in the high temperature components in aerospace structures.

The next topics concerning new polymers are related to Japan's national project led by METI (Ministry of Economics, Trade and Industry) and RIMCOF (Research Institute for Metal and Composites for Future). METI and RIMCOF continue their long-sighted efforts to develop radiation cured resins, their composites and processing technologies to reduce processing costs of composites dramatically [11]. This national project started in fiscal year (FY) 2003 and continues until FY 2007. The annual budget is approximately 600 million JPY and more than 10 companies, four universities and JAXA have joined the project consortium. There are three major targets: the development of radiation cure (or non-heating cure) technologies; development of structural health monitoring technologies; and development of new magnesium alloy technologies. Of course, only the first target has any relationship with the topics in this section. This target is sub-divided into three categories:

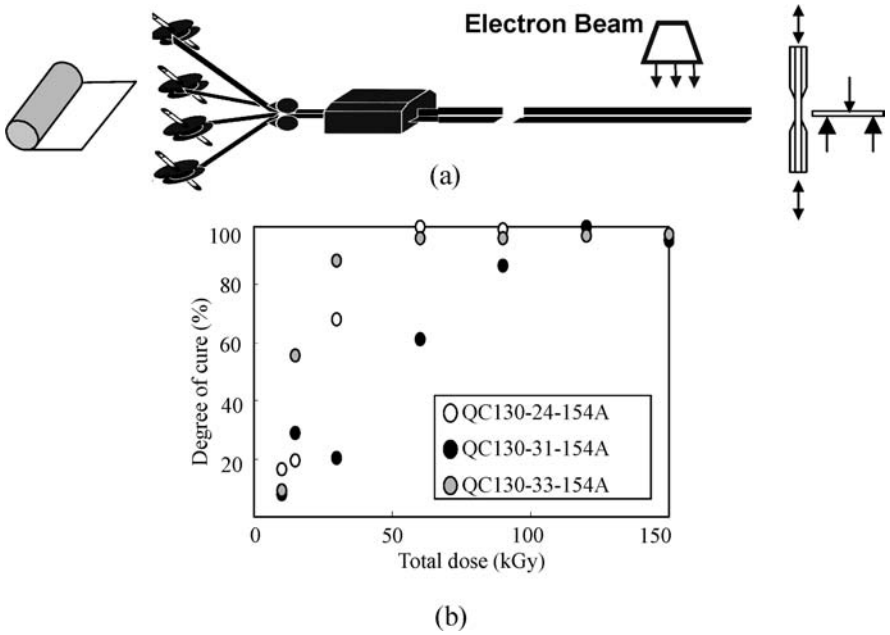

Figure 20. Development of electron beam cure technologies: (a) EBC continuous fabrication system; (b) Cure degree of newly developed prepreg systems.

electron beam curing, ultra-violet curing and visual light curing. Electron beam (EB) curing has some history in research and development in France, Canada, USA and Japan. The pioneering country might be France where they developed technologies for curing some military rocket components and USA is chasing the technology for curing complicated shape composites components of an engine inlet for their fighter aircraft. In the above project, EB curing technology will be combined with a special pultrusion technique [12] developed by Jamco Co. Ltd. and applied to the processing of Airbus A380 composite 2nd floor beams. The long heater portion of this processing system will be replaced by an EB radiation system as shown in Fig. 20a [12]. Optimization of the resin system for obtaining best tack properties and content of cationic photo initiator, and low cost property of epoxy has been carried out [12]. The relationships between the total dose of electron beam and the degree of cure of the developed prepreg systems in this year, QC130-31,33-154A and QC130-24-154A, both developed in FY2001 are shown in Fig. 20b [12]. Although the development of the resin system is virtually complete, much work still remains. The most important task is to reduce the voids formed during the pultrusion process. Some debulk technologies are now under development.

Ultraviolet cure and visual light cure technologies are much more challenging tasks than EB cure. In the general casting technology, ultraviolet curing resin for creating male or female molds is the well established technique, used daily. However, the strength level of such resin for casting is one-tenth or, at best, one-fifth that of a structural epoxy resin. So, a great deal of work is still required

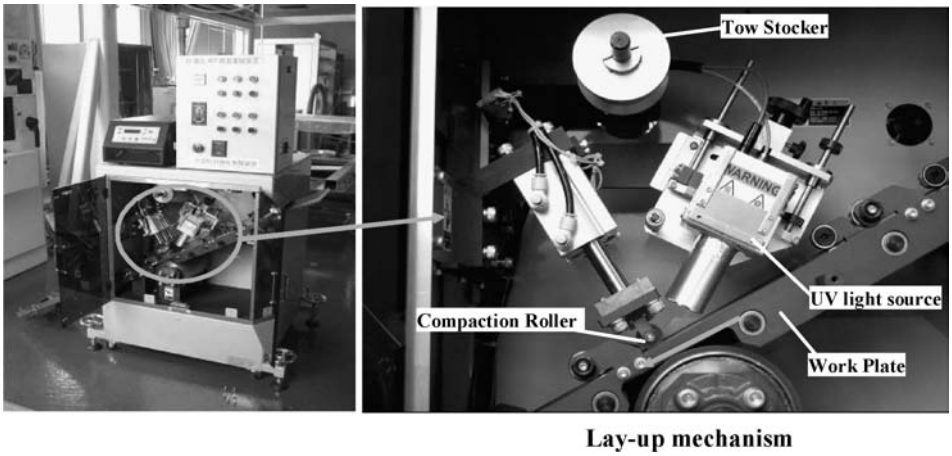

Figure 21. Picture of prototype model of UV cure AFP (Automated Fiber Placement) system.

to develop aircraft level light cured epoxy resin systems. One drawback in carbon epoxy composites (CFRP) is that CFRP is opaque for UV or visible light. Hence, utilization of the heat generated by the curing reaction triggered by UV or light exposure is the key issue in the development. Although a great amount of developmental work still has to be explored, a potential route to successful completion may now be found. Pictures of a prototype model of UV cure AFP (automated fiber placement) system [11] are shown in Fig. 21 where diode type UV light sources are used.

5. DEVELOPMENT OF LOW COST COMPOSITE TECHNOLOGIES

It is well known to the composite communities that the world class new passenger transport plane, Boeing 787, utilizes a large amount of composites for its airframe — almost 50% of its weight empty! A considerable percentage of those composite components, including the main wings and some portion of the fuselage, will be fabricated in Japan. Figure 22 describes the composite application locations in the B-787 and its material weight percentages. However, the baseline composite technology of this airframe remains in prepreg domain. For future aircraft, much lower cost composite technologies will be established. A most promising candidate might be a combination of through-the-thickness reinforcements and liquid resin molding technology, such as resin transfer molding (RTM), vacuum assisted resin transfer molding (VaRTM), or resin film infusion (RFI). In Japan, the first program for developing low cost composite aircraft components technology [13] was operated (1999–2003) by the government owned consortium, Japan Aircraft Development Corporation (JADC). In this program, a 5 m class stub composite wing was fabricated using stitching/RTM stiffeners and co-bond technology with the wing skin. Strength tests including fatigue test of a stiffened panel were successfully

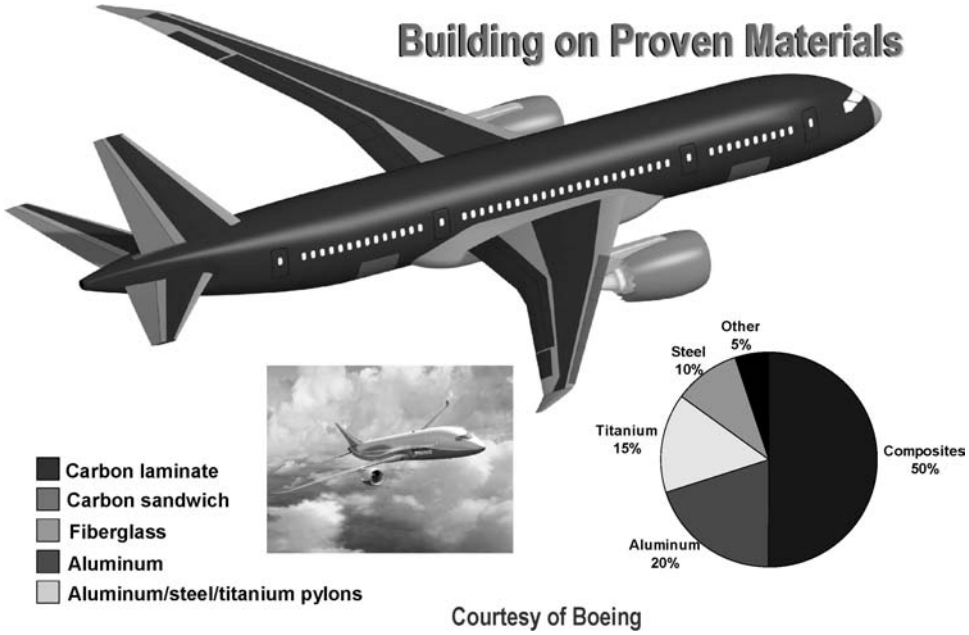

Figure 22. Material fractions and composites application in Boeing B-787.

performed. The second program for low cost composite technology is now being undertaken in ACE TeC/JAXA from 2003 to 2007. In this article, aims, targets and typical results of this newer program and its supporting technologies will be introduced.

The final target of this JAXA program is the actual application of the developed low cost composites technology to Japan's future passenger aircraft. A goal of the cost reduction in this program is indicated in Fig. 23 where a 20% cost reduction than the traditional prepreg route composites is defined as the target. To realize this target, basic and applied research work [14] has been conducted where a combination of the through-the-thickness textile reinforcements and RTM processing is the baseline technology. After the accumulation of such basic knowledge, a considerably large technology verification model of the main wing of 6 m span might be fabricated in FY 2006 and tested in 2007. A conceptual illustration of the planned wing model is shown in Fig. 24. The candidate through-the-thickness reinforcement techniques considered in this JAXA project are Z-anchor® and stitching. Here, a schematic explanation of the Z-anchor® concept [15] is shown in Fig. 25: it is a sort of 'needling' technology rather common in traditional textile fields. By piercing baseline non-crimp fabrics of carbon fiber with special needles a number of times, in-plane fibers are entangled with each other and interlaminar resistance to failure is achieved. Figure 26 [15] indicates the effect of the Z-anchor® on reduction of the delamination area caused by drop weight impacts and, in consequence, upon improvement in compression after impact (CAI)

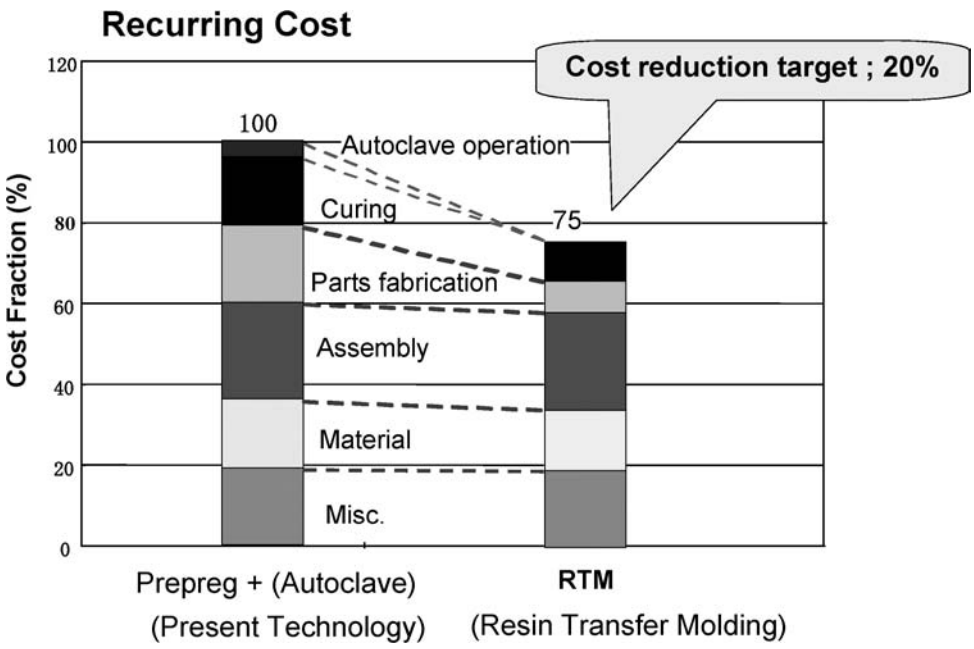

Figure 23. Target of cost reduction in JAXA's low cost composites program.

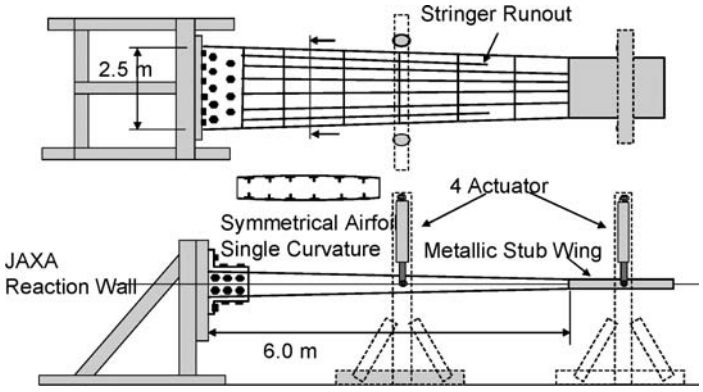

Figure 24. Planned wing box model for low cost composite technology verification in JAXA 5 year project.

strengths. In this figure, Z-Anchor-0 corresponds to the baseline data without the Z-anchor® and Z-Anchor-n corresponds to the cases where n by X times of needling are performed (X is company proprietary information). As indicated, by increasing the numbers of Z-anchor®, the delamination area can be reduced and CAI strength can be increased. However, some level-off trend in CAI strengths can be found between Z-Anchor-2 and Z-Anchor-4. As easily estimated, because a larger number of Z-anchor® times decreases in-plane tensile and compressive strengths, the optimal number of Z-anchor® may exist and it is now under investigation.

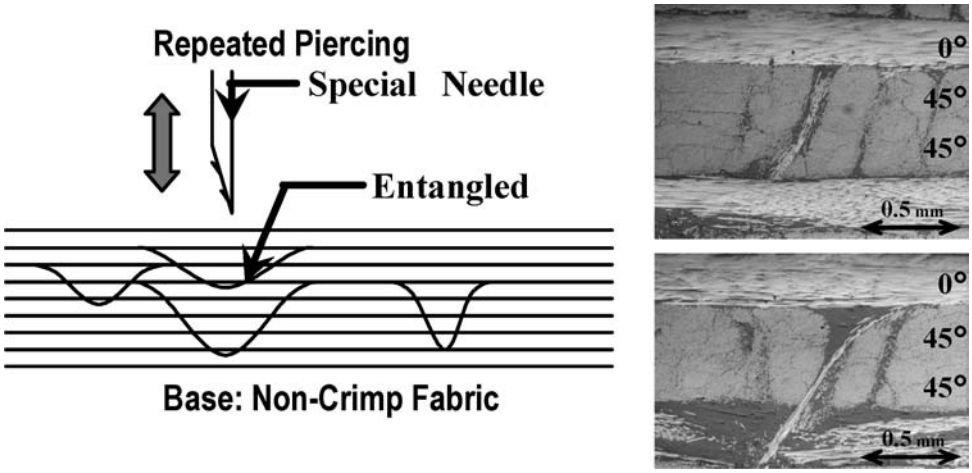

Figure 25. Schematic illustration of Z-anchor® technique for interlaminar reinforcement target: high damage tolerance at low cost.

The second candidate technique for through-the-thickness reinforcement is stitching, which has been studied for a long time. In Japan in the 1980s, NAL reported that stitched CFRP laminates manufactured by prepreg stitch/autoclave consolidation had been evaluated [16]. The results confirmed its ability for crack arresting and to postpone final fracture in static strength. On the other hand, disadvantages such as decline of in-plane and bending strength were admitted. The reason for lower strength was that the stitch needle produced some damage to CF bundles in the prepreg, or voids were formed at the through-the-thickness thread holes. Recently, however, RTM or RFI technique such as dry-preform consolidation system has been refined and the preform damage by stitching could be reduced by using these methods. In the above mentioned low-cost composite research program, interlaminar fracture toughness of stitched laminates has been evaluated and improvement of the numerical model has been pursued. In this research program, stitch threads are mainly Kevlar® and sometimes carbon fibers. Typical results of the measured interlaminar fracture toughness (G_{IC}: Mode I crack energy release rate) of Kevlar® stitched CFRP laminates through double cantilever beam (DCB) specimens and results of numerical simulation [17] are compared in Fig. 27. In order to conduct such DCB tests for stitched specimens, a set of fixtures of an insert tongue was developed by Ishikawa *et al.* with unidirectional CFRP tabs bonded to top and bottom of DCB specimen. Good agreement between the experimental results and the improved numerical predictions using FEM and considering thread pull-out effect explained later is observed in Fig. 27 [17]. Thus, the detailed mechanism of interlaminar fracture toughness improvement by stitching has almost been discovered. From here on, results of the through-the-thickness tension tests using a small square-shaped specimen containing only one stitch point developed by Iwahori [17] are briefly introduced and an establishing process of the improved FEM model consid-

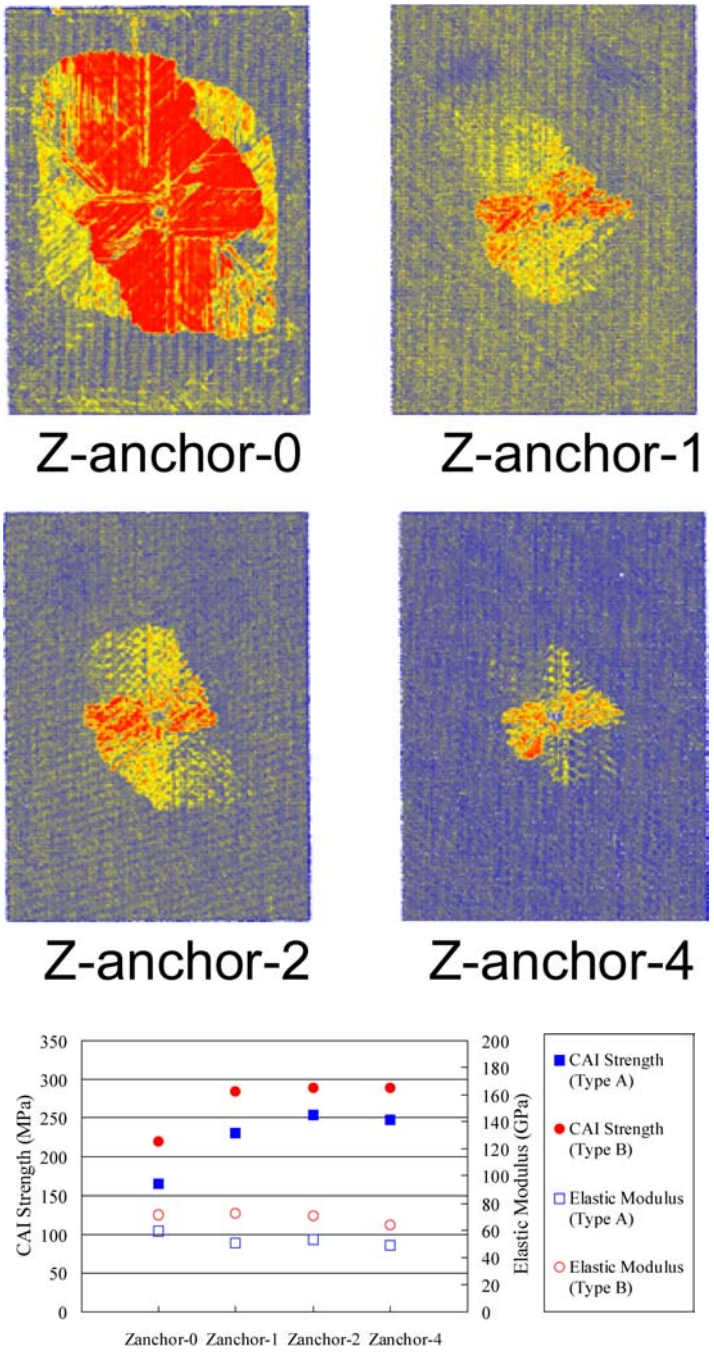

Figure 26. Effect of Z-anchor® on reduction of delamination caused by impact and on increase in compression-after-impact (CAI) strengths.

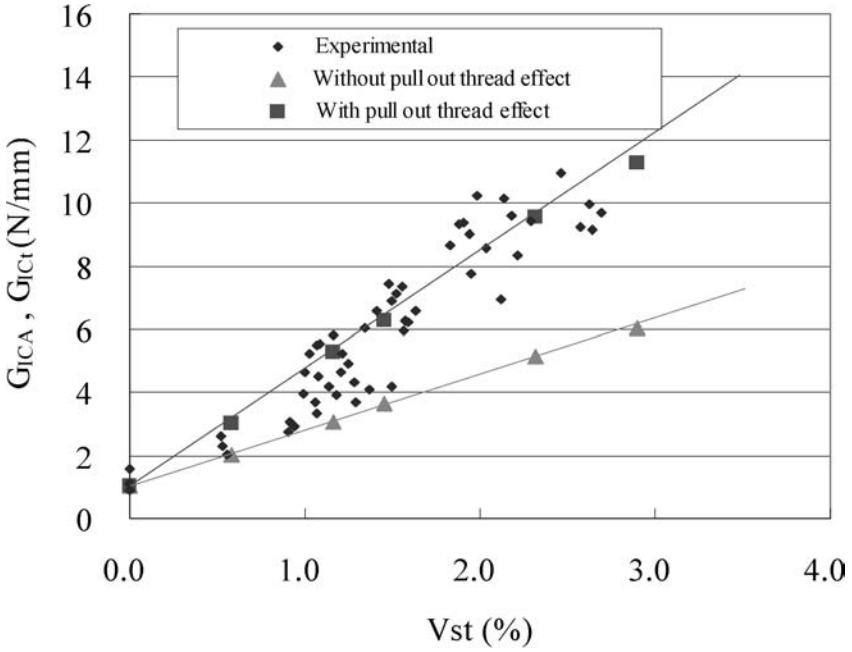

Figure 27. Relationships between Mode I energy release rate (G_{IC}) and volume fraction of stitch thread for CFRP stitched with Kevlar® 29.

ering the thread pull-out effect is also explained. The through-the-thickness tension tests were conducted using a specimen illustrated in Fig. 28a where it was cut out of the stitched CFRP plate and four deep slits were cut in every side surfaces by a diamond wire saw in order to leave one stitch point in the specimen. Figure 28b depicts a picture of the testing set-up of this test using an aluminum T-angle loading tab and the above-mentioned specimen glued to the tab. In some tests, sectional slices were obtained by a micro focus X-ray computed tomography (CT) system along the loading axis at the certain point of displacement. A typical load–displacement curve with the sectional slices by the micro-CT [18] is shown in Fig. 29. Before the initial peak in the load, the composite ligament around the stitch thread does not fail and carries the tension load. After the initial peak, this portion shows the interlaminar fracture while the stitch thread survives and the load once again increases. At the second peak of the load, the stitch thread fails and a sharp drop in the load is shown. After this point, the load–displacement behavior shows a wide variety depending on the location of interlocking point of stitch threads, thickness and material of the threads, while the indicated case shows a thread pull-out where the load decreases gradually. If we count the energy consumed by the threads during this test, we can establish a mechanistic model by modifying the previously constructed simple tuned FEM model. Although the detail of the model theory is not described here, a linear plot in Fig. 27 connecting triangles is the numerical result of the non-pull-out case, which corresponds to a sudden loss of the load after the second peak whereas

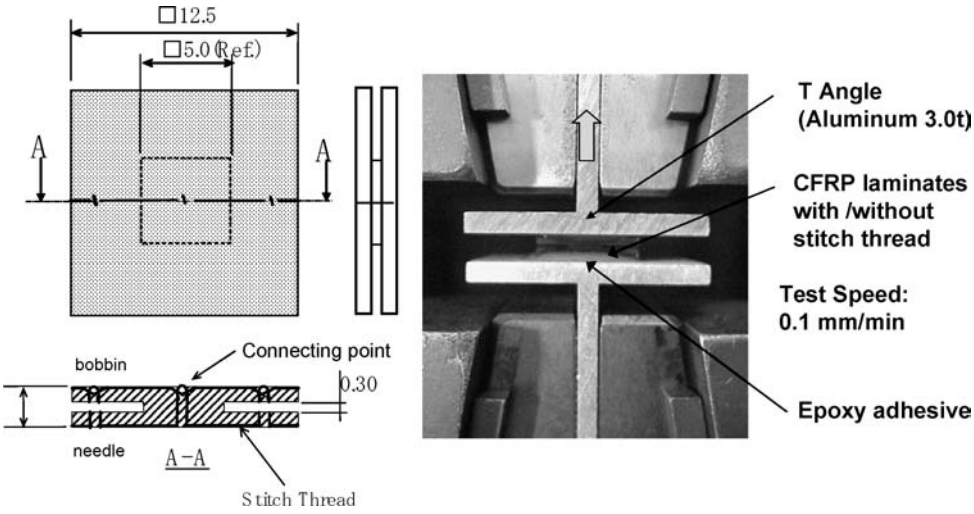

Figure 28. Schematic of through-the-thickness tension test containing one stitch thread. (a) Specimen dimensions. (b) Picture of the test.

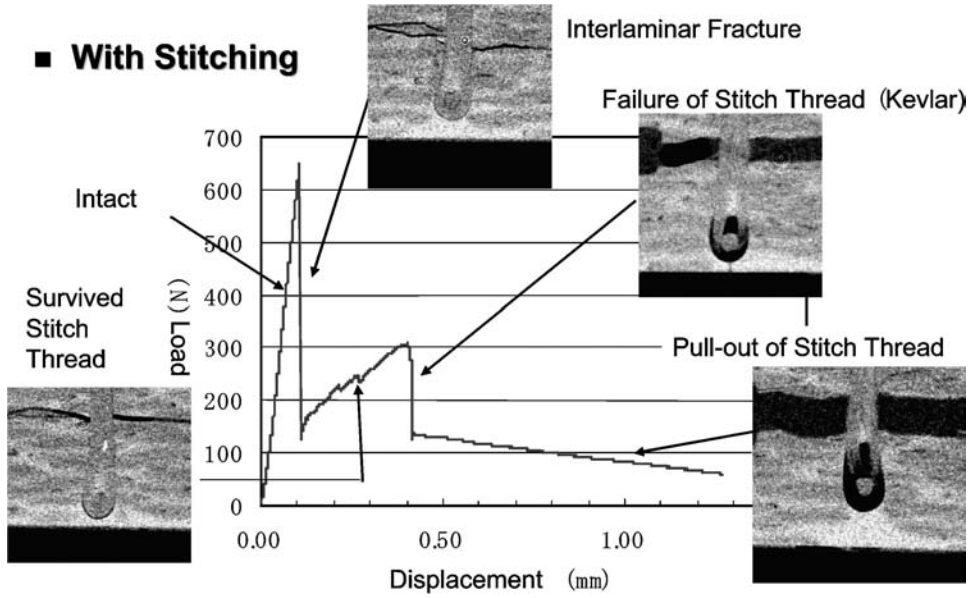

Figure 29. Typical load–displacement curve in through-the-thickness tension test for Kevlar® 29 stitched CFRP: sectional cut by Micro Focus X-Ray CT.

a linear plot connecting squares is the result of pull-out with gradual load decrease. Because the experimental fracture toughness data indicated by small rhombi are obtained from the stitched CFRP laminates by Kevlar®-29 1000 denier thread where the fractured surfaces show much proof debris of the broken thread with long pull-out, good agreement between the experiments and the prediction based on the pull-

out model in Fig. 27 provides enough reason to coincide with each other. Quite detailed information about the interlaminar reinforcement mechanism by stitching is now clarified by the work of Iwahori.

6. REMARKABLE THEORETICAL FINDINGS IN COMPOSITE MECHANICS

In this section, recent remarkable achievements in theoretical contributions to advanced composite research will be reviewed, though a slight bias to the work done in collaboration with the author is inevitable due to his personal knowledge. The first topic here is the work related to a clarification of compression after impact (CAI) behavior. As referred to in the previous section, CAI strength is a key parameter in determination of damage tolerance capability of composites and it affects the determination of design strain factors of composite airframe structures. However, because the mechanics of CAI behavior is an extremely difficult problem due to its non-linear, damage shape-dependent and coupling nature, a full description of its mechanism has not been completed yet. The author believes that a collaborative team of the author's group and Suemasu's group of Sophia University, Tokyo is assuming the closest position to describe the CAI behavior most completely in the world. The author made an overview presentation [19] in the *15th International Conference on Composite Materials (ICCM-15)* and it will be published in a review paper in some composite journal soon. In this article, only two of the remarkable achievements concerning CAI related research will be mentioned.

The first achievement is the development of cohesive zone elements and models using these elements in the finite element analysis of delamination propagation. Schematic illustrations are given in Fig. 30 where the left-top portion shows the idea of two types of elements which can handle opening (Mode-I) and sliding (Mode-II) directions in damage propagations. The key issue in the modeling is the introduction of a smooth function for representing traction–deflection relationships at the interface of two elements [20] as shown in a left-bottom portion in Fig. 30. The peak value of the traction corresponds to the initiation criterion for separation (or delamination) and an approaching phase to zero traction corresponds to the propagation criterion because the energy defined under the curve reaches the critical energy release rate for the further separation. By introducing such a smooth function, it is possible to overcome numerical instabilities, which are very common in these kinds of cohesive zone elements. With the aid of these developed elements, a trial simulation of the DCB test has been conducted and the results are in very good agreement with those obtained by the simple beam theory. Then, the developed models are applied to delamination propagation simulations of a cross-ply laminate [20] of carbon/epoxy, $(0/90/0/90)_{\text{sym.}}$ caused by a static lateral force. Prior to this simulation, similarity in responses of composite plates between by a static indentation force and by an impact which is an actual part of the CAI procedure was confirmed experimentally. Two kinds of models are assumed with

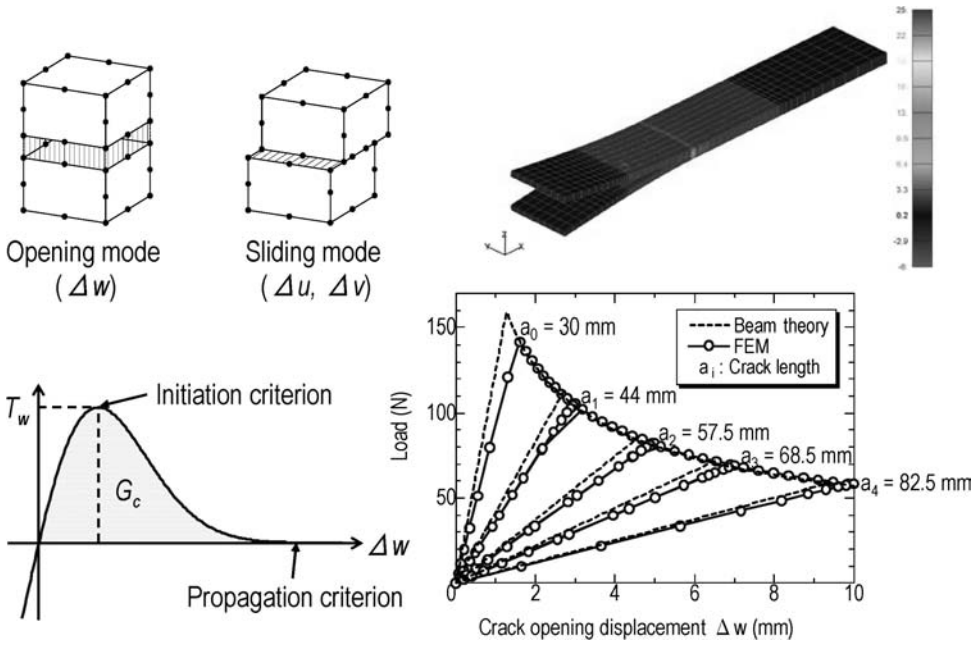

Figure 30. Development of cohesive zone model and trial numerical simulation of DCB test.

and without matrix cracks in 90° layers where they are located at a 45° slant angle as shown in a top portion of Fig. 31 and results are shown in the bottom portion of Fig. 31. Although no significant difference can be observed in load–deflection curves in either of these models, a considerable difference is found in the delamination shapes in each lamina where Model B with matrix cracks gives results that are much closer to the experimental delamination shapes. This work is now being extended to the prediction of the delamination shapes of the quasi-isotropic laminates used in real CAI tests.

The second achievement is also related to this invention of the cohesive zone element. Although Suemasu and the author's group published many remarkable papers predicting the behavior of compressed composite plates by in-plane forces with multiple delaminations [21], they faced a problem in modeling of the delamination propagation which is inevitably caused by a compression load. After the development of the above mentioned model, his group has expanded this idea in order to simulate delamination growth during CAI tests. Model specifications and a finite element model partition are shown in Fig. 32 where the geometrical size of the problem is reduced from no delamination growth cases, e.g. the number of delaminations is 3 instead of 7 in the no-growth case due to the instinctive heavy non-linearity of the problem. Figure 33 depicts delamination growth patterns for the PD30-3D case where delamination growth is considered. In this simulation, the delamination growth takes place just before the peak load, and this finding coincides with the experimental findings reported by the author [22]. The very important is-

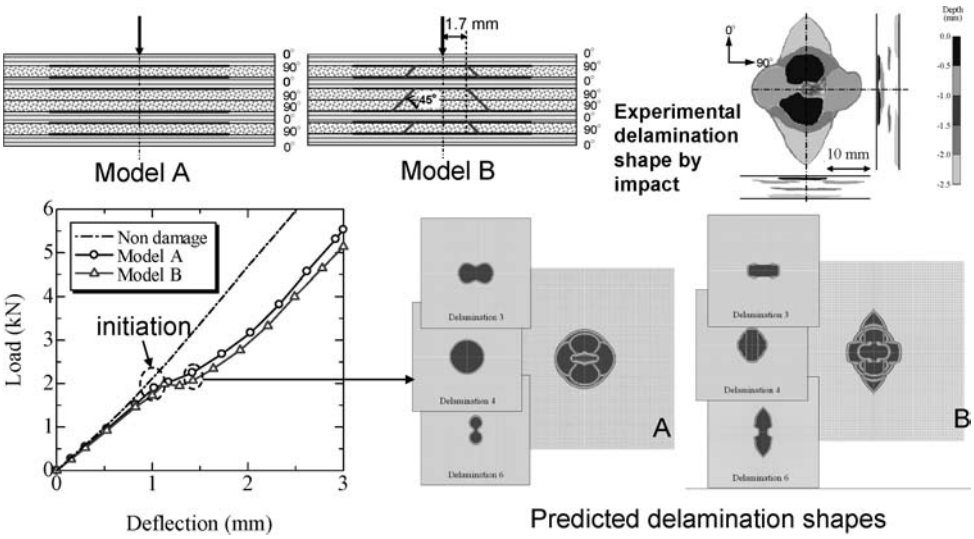

Figure 31. Numerical simulation of delamination propagation of cross-ply laminate using developed cohesive zone model and slant matrix cracks (Model B).

Model	Number of Delaminations	Diameters of Delaminations (mm)
D50-1	**1**	**50**
D30-3S	**3**	**30**
D30-3D	**3**	**25, 30, 35**

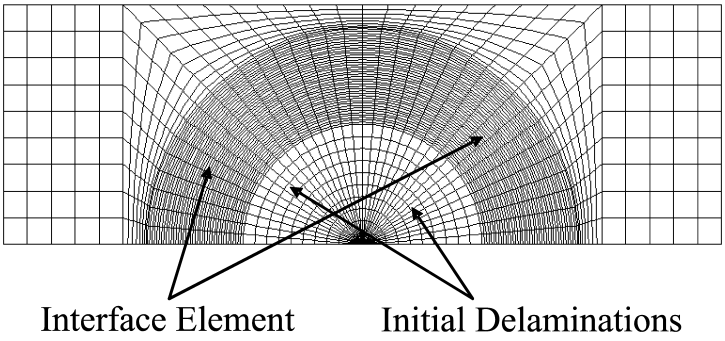

Figure 32. Model specification and finite element analysis model partition for delamination propagation analysis of multiply delaminated carbon epoxy under in-plane compression.

sue appearing in Fig. 33 is the growth of the delamination transverse to the load, which is also the key point in the experimental findings with no exception. Probably, the most important result in the delamination growth analysis is the description of the maximum load as shown in Fig. 34 [19] where PD30-3D indicates the delamination propagation analysis and D30-3D signifiess the same initial geometry and

no growth analysis. No-growth simulation and the no-delamination model behave quite similarly in terms of load *vs.* end-shortening relationships where loads increase continuously. However, the peak load is captured in the case of delamination growth analysis. Although a sudden load drop is described in this case, the other cases of different delamination diameters and shapes lead to gradual decrease of loads. It is very clear that the maximum loads are always identified in all the delamination propagation simulation cases tested. In summary of this important finding,

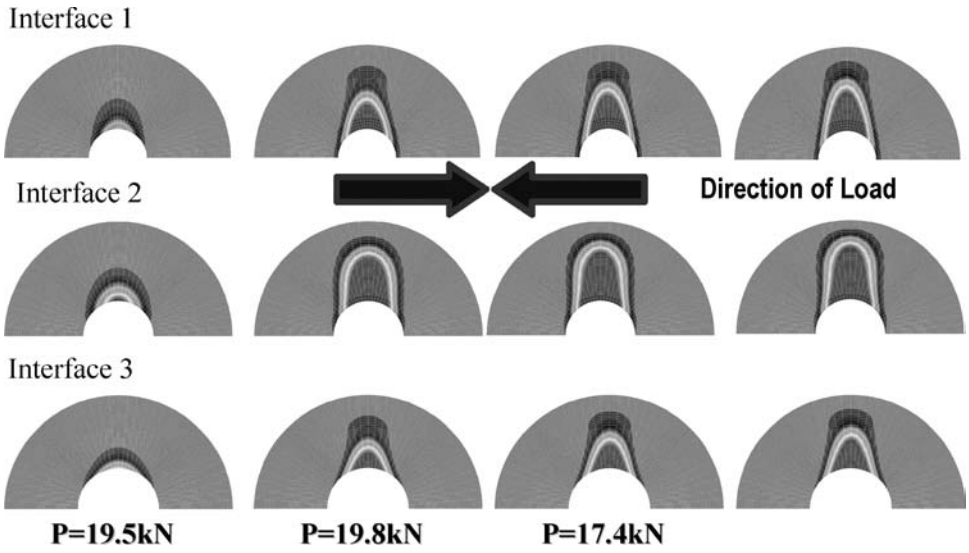

Figure 33. Delamination growth history in model (PD30-3D).

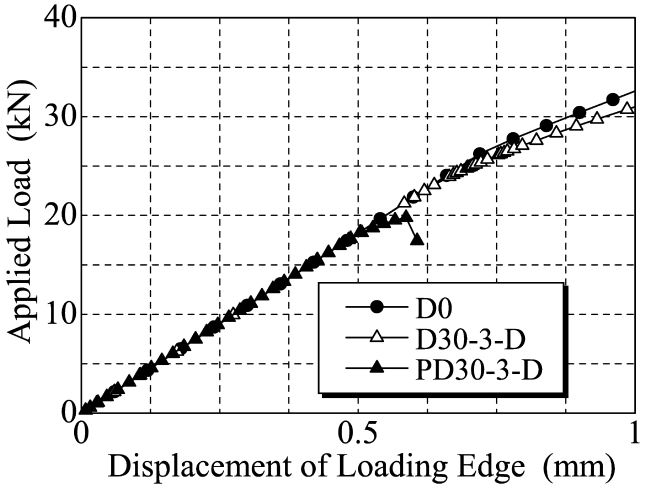

Figure 34. Typical load *vs.* end-shortening curves for no delamination model (D0), no delamination growth model (D30-3D) and delamination growth analysis (PD30-3D).

the following comment can be made. Numerical simulations based on the delamination growth procedure using the cohesive zone element can capture the peak load in the compression, which indicates the CAI strength and predict delamination propagation transversely to the load direction. Now, numerical experiments of multiply delaminated laminates are basically possible if the size of the numerical model is small.

The third theoretical achievement is related to a topic away from the CAI problem. The main body of the topic is related to transverse cracks and cracks generated in the adjacent lamina: an incentive for this research is a cryogenic composite tank for future space transportation systems. A key interest here is a lamina-wise matrix crack accumulation. Only if the matrix cracks are generated in the weakest lamina, e.g. 90° degree ply, is there no gas leakage through such cracks, except for gas permeation inherent in polymer composites. When matrix cracks are generated in adjacent laminae and this process accumulates, direct flow paths of gas will be formed at intersections of cracks and serious leakage will be initiated. Hence, the behavior of matrix crack formation in the laminae adjacent to the initially cracked lamina becomes a very important issue. Yokozeki and Aoki tackled this difficult problem and they published a series of papers; two essential results that they produced are introduced here. The upper portion of Fig. 35 depicts a schematic illustration of the analysis [23], i.e. a two-dimensional shear-lag model based on the oblique coordinates set on a 90/θ imaginary angle ply laminate. Because boundary conditions can easily be written in these oblique coordinates, semi-closed form solutions can be obtained and transformed into the regular orthogonal coordinates.

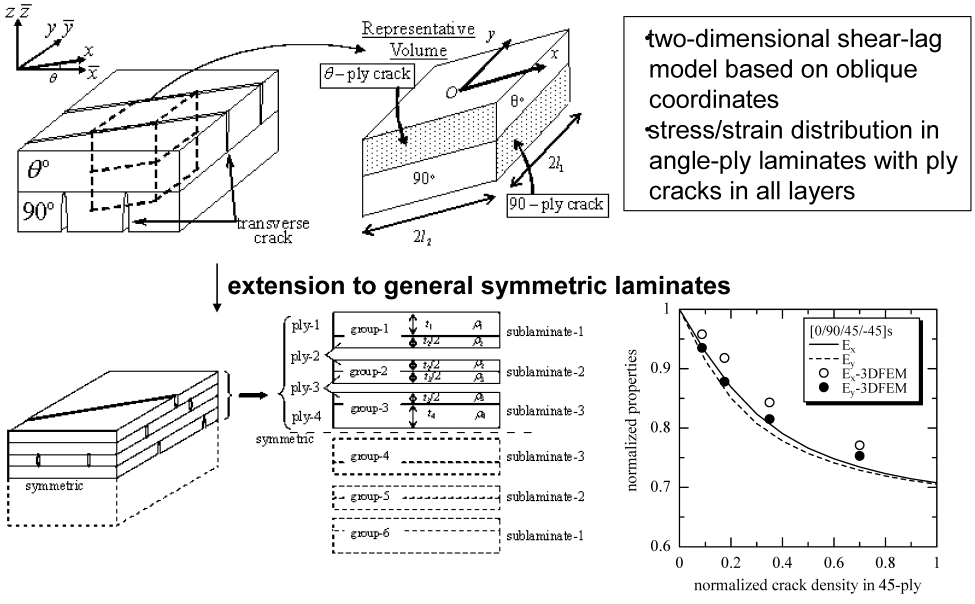

Figure 35. Schematic of stress analysis of symmetric laminates containing obliquely crossed matrix cracks.

Thus, stress–strain distribution in these angle-ply laminates with ply cracks in all layers can be described. By introducing some extra assumptions, this idea can be expanded to solutions for realistic general symmetric laminates as shown in the lower portion of Fig. 35. These semi-closed form solutions in the expression of normalized elastic moduli are compared with results by a 3D finite element analysis and shown in Fig. 35 (lower left) and very good agreement can be observed. Actual experimental demonstration of the mode difference in crack propagation process in plies adjacent to a cracked ply have been conducted in one of their papers [24], as shown in Fig. 36 where unusual unbalanced symmetric laminates of $[0/60_2/90]_s$ and $[0/30_2/90]_s$ are utilized. The former laminate exhibits a damage mode of micro (stitch) crack generation and the latter laminate shows a damage mode of developed crack growth; it is indicated by the analysis that such a mode change depends also on ply thickness. The lower right portion of Fig. 36 depicts a mechanism of the difference in crack growth patterns where 'a' denotes the crack length. In the case of the $[0/60_2/90]_s$ laminate, matrix cracks in the plies adjacent to a cracked ply tend to stop growing due to the drop of the energy release rate by an increase in a, while matrix cracks in the adjacent plies tend to develop in the case of the $[0/30_2/90]_s$ laminate because the G–a curve is flat after its peak [24]. Trends in crack growth captured in the soft X-ray pictures shown in Fig. 36 are well explained by the present analysis [24]. Hence, the basic mechanism of the crack generation and growth

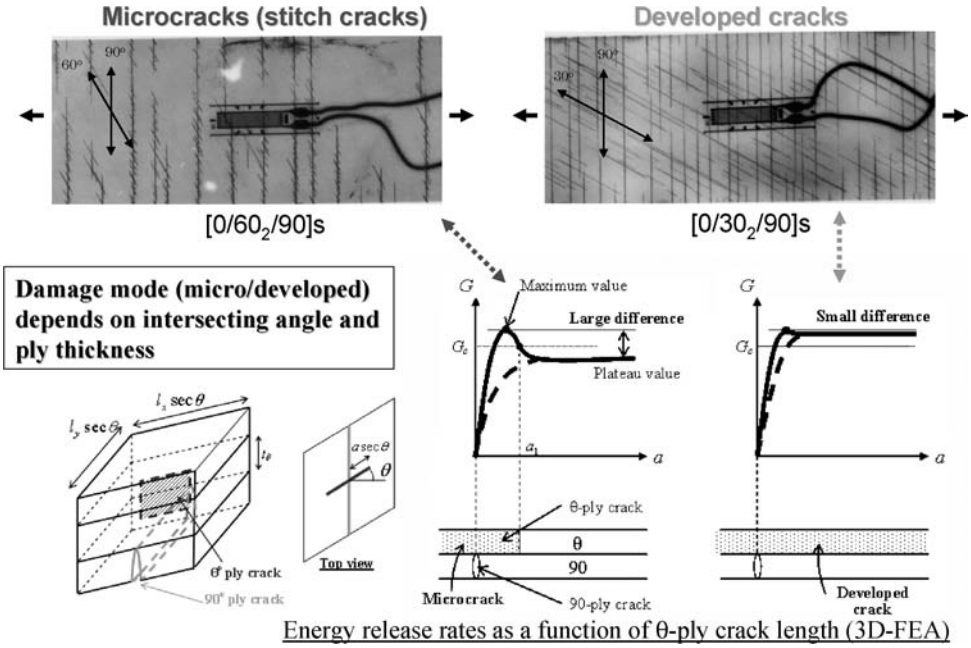

Figure 36. Difference in matrix crack growth pattern in adjacent lamina to initially cracked ply transverse to the main loading.

in the laminae adjacent to the initially cracked ply is greatly clarified and much information for future cryogenic composite tank design is obtained.

The fourth theoretical achievement is related to a technology for structural health monitoring that has a potential to reduce maintenance costs of composite structures. Among several techniques known to the public, optical fiber sensors seem to be the most promising one, in particular, an optical fiber Bragg grating (FBG) sensor is being used for practical applications. FBG sensors (typical gage length: 5–10 mm) have a series of parallel gratings of typical period: 0.5 μm printed into the core of an optical fiber, and a narrow wavelength range of light is reflected from the sensors when a broadband light is illuminated. Since the wavelength at the peak of the reflected signal is proportional to the grating period, the axial strain can be measured through the peak shift. The first important breakthough invented in Japan by Takeda and Hitachi Cable Ltd. is small diameter optical fiber of both of single-mode and multi-mode and its FBG sensor indicated in Fig. 37, left. The invented fiber is 40 μm in cladding diameter and 52 μm in polyimide coating diameter, which is easily embedded within one CFRP ply of typically 125 μm in thickness. Because FBG sensors are very sensitive to non-uniform strain distribution along the entire length of the grating, microscopic damage causing non-uniform strain distribution in CFRP laminates can be detected. Once the fundamental theory of matrix crack detection in cross-ply laminates is established, it can be monitored in general quasi-isotropic laminates [25], as shown in Fig. 37, right. The same principle can be applied to the detection of delamination, which is the most important damage for composite laminates. Figure 38 shows the specimen with an embedded FBG sensor and the experimental results for detection of free-edge delamination in a CFRP $[45/-45/0/90]_s$ laminate [26]. It should be noted that small-diameter optical fibers can be embedded in the laminates and penetrate the surface of the laminates to the outside without introducing any significant defect. The free-edge delamination grew alternatively at 0/90 and 90/0 interfaces under tension–tension fatigue loading.

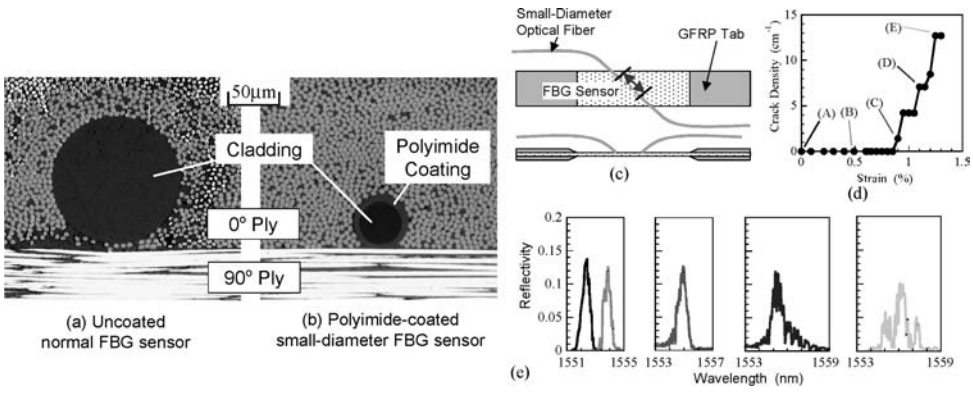

Figure 37. Normal (a) and small-diameter (b) optical fibers embedded in a CFRP lamina (c) $[45/0/-45/90]_s$ CFRP; specimen with embedded small-diameter FBG sensors, (d) transverse crack evolution; (e) change in wavelength distribution of reflected light from FBG sensor.

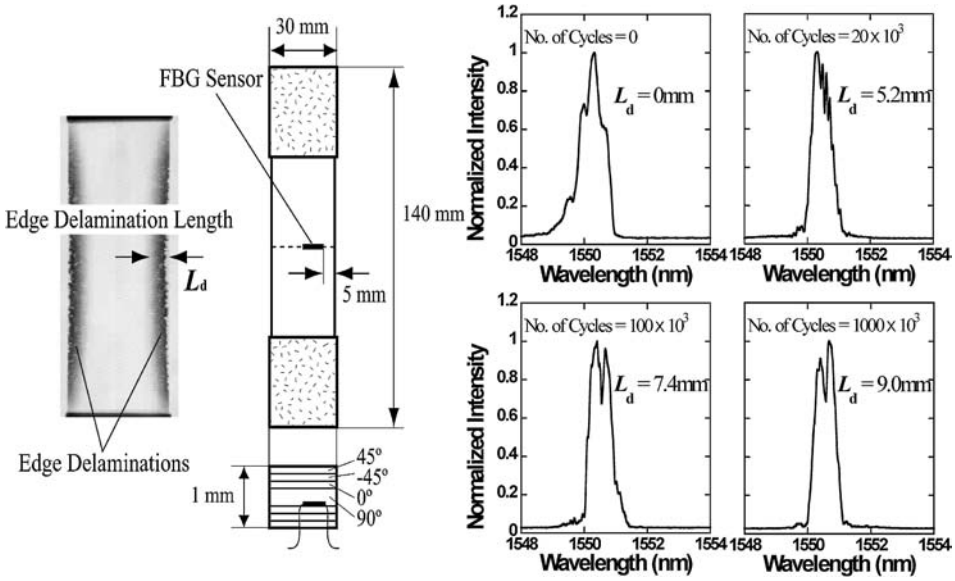

Figure 38. Change in wavelength distribution of reflected light from embedded small-diameter FBG sensor due to edge delamination in $[45/-45/0/90]_s$ CFRP laminate.

An initial single peak in the reflection spectrum was separated into two peaks, and the peak at longer wavelength grew as the edge delamination grew [26]. The two peaks at shorter and longer wavelengths in the reflection spectrum correspond to the strain levels of the bonded and delaminated areas, respectively. This change in the reflection spectrum was found to be well predicted by the theoretical prediction [26]. This technique can also be applied to other types of delamination detection around stress-concentrated regions such as rivet holes.

7. CONCLUSIONS

Recent activities in advanced composites technology developments conducted in Japan are reviewed based on the author's knowledge in the two directions of basic research and engineering applications.

New topics in reinforcing fibers that are described include low modulus pitch-based carbon fiber and PBO fiber. The second subject related to reinforcement is very topical and includes nano-technology based composites using materials such as carbon nano-tube, or carbon nano-fiber, or nano-clay. The most remarkable outcome in this field at present is a compression strength improvement by blending cup-stack type carbon nano-fiber (CSNF) into epoxy matrix. Prepreg containing this CSNF has been developed and has already been released into the market.

The third topic is related to newly developed high performance polymers including heat resistant polyimide, Tri A-PI, and its family. The most recent product is a heat resistant polyimide that is highly soluble in some organic solvents, which is

suitable for preparation of imide wet prepreg. Composites fabricated through this prepreg route exhibit no voids and defects compared to the traditional amid-acid polyimide prepreg route. Another new topic in polymer technology is related to Japan's national project where radiation cure polymers and their processing have been pursued. Electron beam cure, ultra-violet cure and visual light cure resins and their processing technologies have been developed in this national project.

The next topic is the development of the low cost composites technology mainly for aircraft components. JAXA's activities related to this field are introduced first, based on two new key textile technologies, Z-anchor® and stitching. New findings about the mechanism of interlaminar reinforcement by stitching are dealt with briefly in the introduction.

Finally, remarkable theoretical findings about composite mechanics in recent years in Japan are introduced briefly. A clarification of mechanics of compression after impact behavior by using the newly developed cohesive zone element is reviewed first. Numerical simulations based on the delamination growth procedure using the cohesive zone element can capture the peak load in the compression, which indicates the CAI strength and predicts delamination propagation transversely to the load direction. Matrix crack growth theories in the laminae adjacent to the initially cracked layer are introduced next where an incentive of this research is the development of a cryogenic composite tank for future space transportation systems. The final topic is the development of the theory of structural health monitoring by using small diameter FBG sensors. By further evolution of these theories, structural health monitoring will approach the level where it will be suitable for use in practical applications.

REFERENCES

1. Y. Arai, Current status and future of pitch based carbon fiber, *Proc. 18th Composite Material Seminar*, pp. 9–16. The Japan Carbon Fiber Manufacturing Association, Tokyo (2005) (in Japanese).
2. S. Takemura, M. Mizuta and A. S. Kobayashi, Improvement of impact bending properties of golf shaft made of carbon fiber reinforced composites by application of low modulus pitch-based carbon fiber, *J. Japan Soc. Compos. Mater.* **31**, 120–127 (2005) (in Japanese).
3. Z. Wu, K. Iwashita, K. Hayashi, T. Higuchi, S. Murakami and Y. Koseki, Strengthening prestressed-concrete girders with externally prestressed PBO fiber reinforced polymer sheets, *J. Reinforced Plastics and Compos.* **22**, 1269–1285 (2003).
4. Z. Wu, K. Iwashita, K. Hayashi, T. Higuchi, S. Murakami and Y. Koseki, Upgrading method of RC flexural structures with externally prestressed PBO fiber sheets, *J. Japan Soc. Compos. Mater.* **28**, 146–155 (2002) (in Japanese).
5. Y. Iwahori, S. Ishiwata, T. Sumizawa and T. Ishikawa, Mechanical properties improvement in two phase and three phase composites using carbon nano fiber dispersed resin, *Composites: Part A* **36**, 1430–1439 (2005).
6. S. Ishiwata, T. Yanagisawa, T. Ishikawa and Y. Iwahori, Reinforcement of CFRP by Cup-Stacked Type Carbon Nanotube, in: *Proceedings of 30th Composites Symposium*, pp. 275–276. The Japan Society for Composite Materials, Matsuyama, Japan (2005).

7. T. Ogasawara, Y. Ishida, T. Ishikawa and R. Yokota, Characterization of multi-walled carbon nanotube/phenylethynyl terminated polyimide composites, *Composites: Part A* **34**, 67–74 (2004).
8. T. Ogasawara, Y. Ishida, T. Ishikawa, T. Aoki and T. Ogura, Helium gas permeability of montmorillonite/epoxy nanocomposites, *Composites: Part A* (in press).
9. R. Yokota, S. Yamamoto, S. Yano, T. Sawaguchi, M. Hasegawa, H. Yamaguchi, H. Ozawa and R. Sato, Molecular design of heat resistant polyimides having excellent processability and high glass transition temperature, *High Perform. Polym.* **13**, S61–S72 (2001).
10. Y. Ishida, T. Ogasawara and R. Yokota, Development of highly soluble addition-type imide oligomers, imide wet prepregs and polyimide/CF composites, in: *Proceedings of SAMPE 2005 Fall Conference*, SAMPE, Seattle, USA, CD-ROM (2005).
11. T. Ishikawa, Y. Yamaguchi and M. Noda, Introduction of new project for manufacturing and processing of aircraft components for future generation, *J. Japan Soc. Compos. Mater.* **31**, 101–111 (2005) (in Japanese).
12. J. Gotoh, T. Hasegawa, M. Yoda and M. Imuta, Development of electron beam processing for aircraft structures, in: *Proceedings of 2005 JSASS-KSAS Joint International Symposium on Aerospace Engineering*, JSASS, Nagoya, Japan, CD-ROM (2005).
13. T. Ishikawa, Y. Iwahori, Y. Aoki, S. Takeda and H. Kikukawa, Research work for strength evaluation of composites structure fabricated by new RTM technology, *J. Japan Soc. Aeronaut. Space Sci.* **53**, 28–33 (2005) (in Japanese).
14. T. Ishikawa, Overview of low-cost composite technology in Japan (JAXA), in: *Proceedings of 2004 KSAS-JSASS Joint Symposium on Aerospace Engineering*, Korea Society for Aerospace Science, Seoul, Korea, CD-ROM (2004).
15. Y. Iwahori, K. Yamada, Y. Ishibashi, F. Takeda, T. Ishikawa and G. Ben, Interlaminar strength improvement for CFRP laminates by Z-anchor® technology, in: *Proceedings of 15th International Conference on Composite Materials (ICCM-15)*, Durban, South Africa, CD-ROM (2005).
16. Y. Tada and T. Ishikawa, Experimental evaluation of the effects of stitching on CFRP laminate specimens with various shapes and locations, *Key Engineering Materials* **37**, 305–316 (1989).
17. Y. Iwahori, S. Sugimoto, Y. Hayashi, S. Horikawa, T. Ishikawa and H. Fukuda, Research of through-the-thickness tensile strength properties by tensile tests in the stitching direction for stitched CFRP laminates, *J. Japan Soc. Compos. Mater.* **32**, 2–31 (2006) (in Japanese).
18. Y. Iwahori, S. Sugimoto, T. Kato and T. Ishikawa, Mechanism of interlaminar strength improvement for CFRP laminates by stitching, in: *Proceedings of SAMPE Europe 26th International Conference and Forums*, Paris, France, pp. 171–176 (2005).
19. T. Ishikawa, Y. Aoki and H. Suemasu, Pursuit of mechanical behavior in compression after impact (CAI) and open hole compression (OHC), in: *Proceedings of 15th International Conference on Composite Materials (ICCM-15)*, Durban, South Africa, CD-ROM (2005).
20. Y. Aoki, H. Suemasu and T. Ishikawa, Damage propagation in CFRP laminates subjected to low velocity impact and static indentation, *Adv. Composite Mater.* **21** (to be published).
21. H. Suemasu, T. Irie and T. Ishikawa, Compressive behavior of laminated composites with multiple delaminations, in: *Proceedings of the Fifth Joint Canada-Japan Workshop on Composites*, Yonezawa, Japan, D E Stech Publications, Inc., pp. 433–440 (2004).
22. T. Ishikawa, S. Sugimoto, M. Matsushima and Y. Hayashi, Some experimental findings in compression-after-impact (CAI) tests of CF/PEEK (APC-2) and conventional CF/epoxy flat plates, *Compos. Sci. Technol.* **55**, 349–363 (1995).
23. T. Yokozeki and T. Aoki, Overall thermoelastic properties of symmetric laminates containing obliquely-crossed matrix cracks, *Compos. Sci. Technol.* **65**, 1647–1654 (2005).

24. T. Yokozeki, T. Aoki, T. Ogasawara and T. Ishikawa, Effects of layup angle and ply thickness on matrix crack interaction in contiguous plies of composite laminates, *Composites: Part-A* **36**, 1229–1235 (2005).
25. T. Mizutani, Y. Okabe and N. Takeda, Quantitative evaluation of transverse cracks in carbon fiber reinforced plastic quasi-isotropic laminates with embedded small-diameter fiber Bragg grating sensors, *Smart Mater. Struct.* **12**, 898–903 (2003).
26. S. Takeda, Y. Okabe, T. Yamamoto and N. Takeda, Detection of edge delamination in CFRP laminates under cyclic loading using small-diameter FBG sensors, *Compos. Sci. Technol.* **63**, 1885–1894 (2003).